MAY 16 2000

0830-L-02 NASI.29/3-2:00-05

NASA TechBriefs

National Aeronautics and
Space Administration

Electronic Components and Circuits

Electronic Systems

Physical Sciences

Materials

Computer Programs

Mechanics

Machinery

Fabrication Technology

Mathematics and Information Sciences

Life Sciences

Ann 2000 0/8639

C

INTRODUCTION

Tech Briefs are short announcements of innovations originating from research and development activities of the National Aeronautics and Space Administration. They emphasize information considered likely to be transferable across industrial, regional, or disciplinary lines and are issued to encourage commercial application.

Availability of NASA Tech Briefs and TSPs

Requests for individual Tech Briefs or for Technical Support Packages (TSPs) announced herein should be addressed to

National Technology Transfer Center
Telephone No. **(800) 678-6882** or via World Wide Web at **www2.nttc.edu/leads/**

Please reference the control numbers appearing at the end of each Tech Brief. Information on NASA's Commercial Technology Team, its documents, and services is also available at the same facility or on the World Wide Web at **www.nctn.hq.nasa.gov**.

Commercial Technology Offices and Patent Counsels are located at NASA field centers to provide technology-transfer access to industrial users. Inquiries can be made by contacting NASA field centers and program offices listed below.

NASA Field Centers and Program Offices

Ames Research Center
Carolina Blake
(650) 604-0893 or
cblake@mail.arc.nasa.gov

Dryden Flight Research Center
Lee Duke
(805) 258-3802 or
lee.duke@dfrc.nasa.gov

Goddard Space Flight Center
George Alcorn
(301) 286-5810 or
galcorn@gsfc.nasa.gov

Jet Propulsion Laboratory
Merle McKenzie
(818) 354-2577 or
merle.mckenzie@comail.jpl.nasa.gov

Johnson Space Center
Hank Davis
(281) 483-0474 or
hdavis@gp101.jsc.nasa.gov

John F. Kennedy Space Center
Gale Allen
(407) 867-6626 or
galeallen-1@ksc.nasa.gov

Langley Research Center
Dr. Joseph S. Heyman
(804) 864-6006 or
j.s.heyman@larc.nasa.gov

Glenn Research Center
Larry Viterna
(216) 433-3484 or
cto@lerc.nasa.gov

George C. Marshall Space Flight Center
Sally Little
(256) 544-4266 or
sally.little@msfc.nasa.gov

John C. Stennis Space Center
Kirk Sharp
(228) 688-1929 or
ksharp@ssc.nasa.gov

NASA Program Offices
At NASA Headquarters there are seven major program offices that develop and oversee technology projects of potential interest to industry:

Carl Ray
Small Business Innovation Research Program (SBIR) & Small Business Technology Transfer Program (STTR)
(202) 358-4652 or
cray@mail.hq.nasa.gov

Dr. Robert Norwood
Office of Aeronautics and Space Transportation Technology (Code R)
(202) 358-2320 or
rnorwood@mail.hq.nasa.gov

John Mulcahy
Office of Space Flight (Code MP)
(202) 358-1401 or
jmulcahy@mail.hq.nasa.gov

Gerald Johnson
Office of Aeronautics (Code R)
(202) 358-4711 or
g.johnson@aeromail.hq.nasa.gov

Bill Smith
Office of Space Science (Code S)
(202) 358-2473 or
wsmith@sm.ms.ossa.hq.nasa.gov

Roger Crouch
Office of Microgravity Science Applications (Code U)
(202) 358-0689 or
rcrouch@hq.nasa.gov

Granville Paules
Office of Mission to Planet Earth (Code Y)
(202) 358-0706 or
gpaules@mtpe.hq.nasa.gov

BLANK PAGE

NASA TechBriefs

National Aeronautics and Space Administration

May 2000
00-05

5 Electronic Components and Circuits

11 Electronic Systems

15 Physical Sciences

27 Materials

33 Mechanics

37 Fabrication Technology

41 Mathematics and Information Sciences

This document was prepared under the sponsorship of the National Aeronautics and Space Administration. Neither the United States Government nor any person acting on behalf of the United States Government assumes any liability resulting from the use of the information contained in this document, or warrants that such use will be free from privately owned rights.

BLANK PAGE

Electronic Components and Circuits

Hardware, Techniques, and Processes

7 Submillimeter-Sized $Bi_{2-x}Sb_xTe_3$ Thermoelectric Devices
8 On-Chip Correction for Defective Pixels in an Image Sensor
9 Magnetoelectric Sensors and Electric Generators
9 High-Speed Complex-Amplitude Liquid-Crystal SLMs

BLANK PAGE

Submillimeter-Sized $Bi_{2-x}Sb_xTe_3$ Thermoelectric Devices

Electrochemical deposition is the key to mass-producibility.

NASA's Jet Propulsion Laboratory, Pasadena, California

Submillimeter-sized thermoelectric devices based on thick films of $Bi_{2-x}Sb_xTe_3$ are undergoing development. As electronic circuits are designed with ever greater packaging densities and power densities, there is an increasing need for small thermoelectric devices to provide active spot cooling for power amplifiers and other heat-generating electronic components. $Bi_{2-x}Sb_xTe_3$ is the preferred thermoelectric material for the operational temperature range (<200 °C) of typical advanced microelectronic components. $Bi_{2-x}Sb_xTe_3$ thermoelectric devices could also be used as electric-power generators; moreover, because of the smallness of the thermoelectric legs in these devices, the numbers of legs can be of the order of 100 times those of conventional bulk thermoelectric devices, making it possible to generate higher potentials (of the order of 100 V), that are more compatible with other electronic components.

The figure depicts a representative device of this type, wherein the $Bi_{2-x}Sb_xTe_3$ thermoelectric legs have lengths, widths, and thicknesses of the order of tens of microns. The thermoelectric legs are integrated with contact, diffusion-barrier, and electrode layers, all sandwiched between two thermally conductive, electrically insulating outer layers (made of AlN or synthetic diamond substrates) that are placed in contact with the heat source and heat sink, respectively. The $Bi_{2-x}Sb_xTe_3$ legs are made by electrochemical deposition from an aqueous solution; the other parts of the device are fabricated by various conventional integrated-circuit-fabrication techniques, including photolithography and vacuum deposition.

In comparison with such conventional semiconductor-fabrication techniques as sputter deposition, vacuum evaporation, and chemical vapor deposition (CVD), electrochemical deposition offers several advantages for fabrication of the $Bi_{2-x}Sb_xTe_3$ thermoelectric legs. Growth rates achievable by electrochemical deposition are in the range of tens of microns per hour — fast enough for mass production of devices in the desired size range — whereas lower growth rates achievable by the conventional techniques are better suited to fabrication of submicron-sized devices. The conventional techniques are poorly suited to fabrication of $Bi_{2-x}Sb_xTe_3$ devices because the vapor pressures of Bi, Sb, and Te are very different; on the other hand, the compositions of films grown by electrochemical deposition can be controlled via the concentrations of the constituents of the aqueous deposition solutions.

Substrates can be coated with metal interconnection busses and contact pads and then masked, all by conventional integrated-circuit-fabrication techniques. Then $Bi_{2-x}Sb_xTe_3$ thermoelectric legs can be electrodeposited onto the contact pads through the holes in the masks. Thus, conventional integrated-circuit-fabrication techniques can readily be combined with electrochemical deposition for mass production of submillimeter $Bi_{2-x}Sb_xTe_3$ thermoelectric devices.

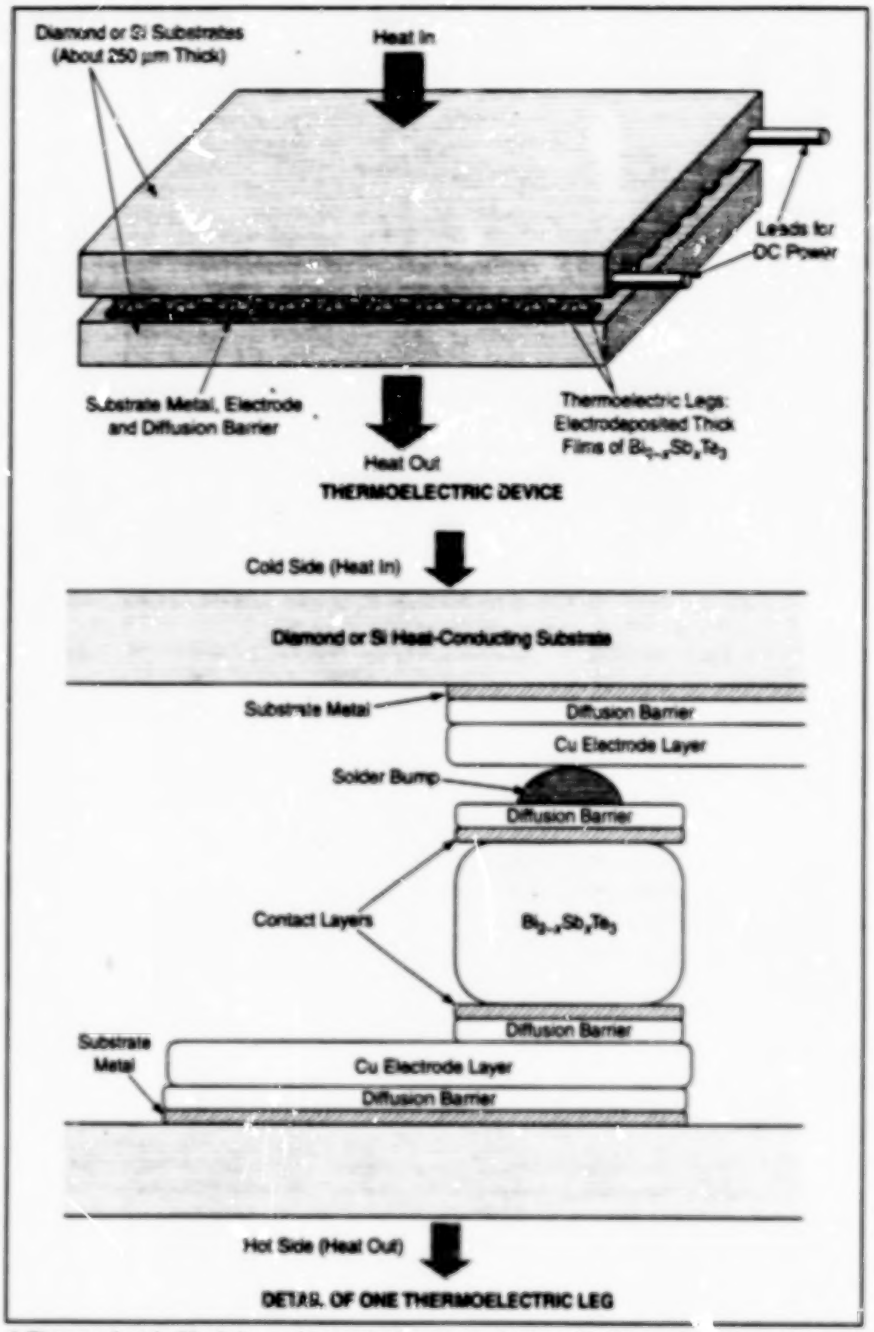

A Thermoelectric Module would contain thermoelectric legs made from thick films of n- and p-doped $Bi_{2-x}Sb_xTe_3$, plus multiple metal layers and outer layers made from high-thermal-conductivity materials. The thermoelectric legs would be connected electrically in series and thermally in parallel.

A significant part of the development effort thus far has been devoted to the electrochemical deposition process. The general approach is to dissolve Bi, Sb, and Te in nitric acid, then put the resulting solution in an electrochemical cell, wherein $Bi_{2-x}Sb_xTe_3$ (which is insoluble in HNO_3) is deposited on a cathode. Process parameters that must be optimized include the pH of the solution; the concentrations of Bi, Sb, and Te in the solution; the temperature of the solution; stirring of the solution; the deposition voltage and current density; the surface finish of the cathode; and post-deposition annealing. One of findings of experiments conducted thus far is that the limited solubility of Sb in the solution can be enhanced by use of tartaric acid as a buffer.

This work was done by Jean-Pierre Fleurial, Margaret A. Ryan, Alex Borshchevsky, Wayne Phillips, Elizabeth Kolawa, G. Jeffrey Snyder, and Thierry Caillat of Caltech for **NASA's Jet Propulsion Laboratory**. *Further information is contained in a TSP (see page 1).*
NPO-20...

On-Chip Correction for Defective Pixels in an Image Sensor

Readouts from nearest neighbors could be substituted for defective pixels.

Lyndon B. Johnson Space Center, Houston, Texas

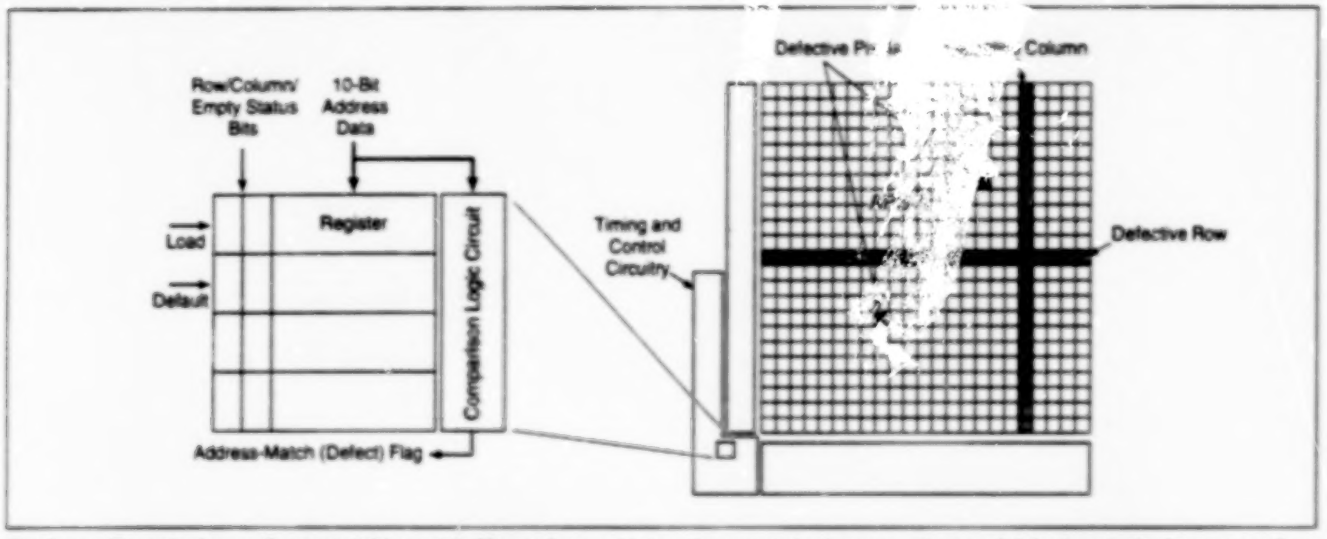

Registers Functioning as Content-Addressable Memories would store the row and column coordinates of defective pixels. As many as four addresses, each 10 bits wide, could be stored for identifying defective individual pixels or defective entire rows or columns of pixels.

A method of correcting for defective pixels in an integrated-circuit image sensor of the active-pixel sensor (APS) type has been proposed. The corrections would be made by additional readout circuitry on the image-sensor chips. By making it unnecessary to discard sensor chips that contain limited numbers of scattered defects, the method would increase effective production yields and thereby lower the costs of individual image sensors.

Two issues arise in trying to correct for defective pixels: how to store information on the locations of these pixels and how to process pixel outputs in the readout process. Because most of the area of an image-sensor chip is occupied by the array of pixels, there is little room for circuitry for storing addresses of defective pixels. Accordingly, the coordinates of any defective pixels and of any defective entire rows or columns of pixels would be stored in several registers (see figure), the number of registers being based on a practical upper bound on the number of pixels, rows, or columns likely to be defective. In the initial proposed design, there would be four such registers, and they would be embedded in the on-chip timing and control circuitry.

The set of registers would function in the manner of a content-addressable memory. During readout, the current row and/or column address would be applied to this memory and a flag would be generated if the current address matched the stored address, signifying that the current pixel, row, or column is defective.

The method admits of alternative designs corresponding to alternative ways to respond to a "defect" flag. The simplest approach is to design the readout control logic circuit to simply skip an entire row that contains even one bad pixel, skip an entire bad column, and increment to the next row or column. In this approach, it would suffice to store only the row address of a single bad pixel.

Another approach would involve substituting, for each defective pixel, the average of readouts from the eight surrounding pixels. This approach would be less practical or attractive for on-chip implementation because it would necessitate more circuitry occupying more chip area. The additional circuitry would be necessary for storing information from three rows at a time (the previous row, the current row, and the next row to be read out) plus processing of information from three rows and columns at a time.

A more practical approach would involve replacing the output from a dead pixel with a copy of the output from a neighboring pixel that was read out previously. The copy could be obtained by use of a simple single-pixel delay line.

An essential step in this method would be a procedure for testing to locate defective pixels, rows, and columns and for writing the addresses of these pixels, rows, and columns in the registers. In the first generation of image sensors designed according to this method, the testing and the programming of registers would probably be performed manually. Eventually, it should be possible to add automated testing and programming circuitry to the chips.

This work was done by Sabbas Doudoumopoulos, Roger Panicucci, and Eric H. Fossum of Photobit for **Johnson Space Center**.
MSC-22827

Magnetoelectric Sensors and Electric Generators

Novel applications of the magnetoelectric effect are proposed.

NASA's Jet Propulsion Laboratory, Pasadena, California

Electric generators and magnetic-field sensors of a proposed type would be based on the magnetoelectric effect. A simple device of this type (see figure) would consist mainly of an inner layer of a magnetoelectric material sandwiched between two outer layers of a ferromagnetic material. Electrical contacts would be placed at opposite ends of the magnetoelectric material.

As its name suggests, a magnetoelectric material is one that exhibits the magnetoelectric effect, which is a linear coupling between magnetization and electric polarization. The polarization electric field is perpendicular to the magnetic induction vector and its magnitude is proportional to the strength of the magnetic induction vector.

The electrical contacts could be used to connect the ends of the magnetoelectric layer to a voltmeter or other suitable instrument for measuring changes in the polarization electric charge. The voltage reading would be proportional to the change in the charge and thus to the change in the polarization electric field and thus, further, to change in the magnetic induction. Operated in this way, the device could be used as a magnetic-field sensor.

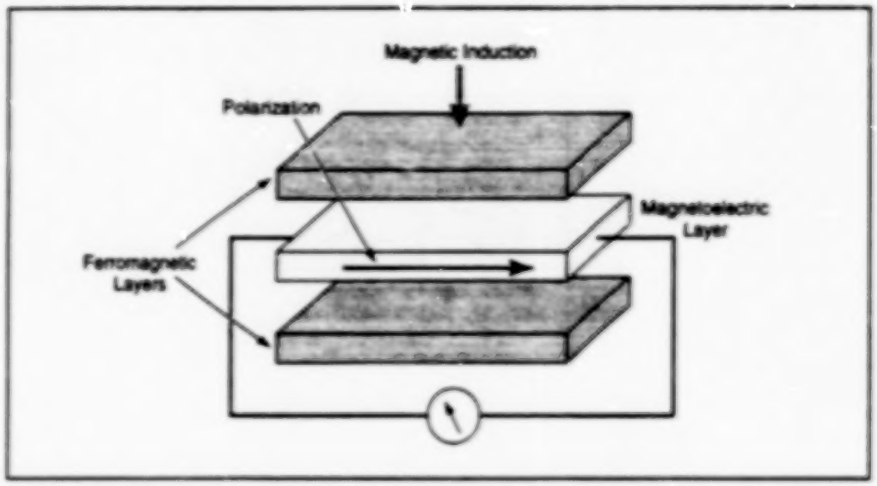

The Sandwichlike Device could be used to sense or to extract power from a varying magnetic field.

If the ends of the magnetoelectric layer were connected to suitable external circuitry and the magnetic field varied, then a sustained electrical current would flow. Operated in this way, the device could be used to sense or to extract power from a strongly varying magnetic field.

This work was done by Julian Blosiu and Mary Boghosian of Caltech for **NASA's Jet Propulsion Laboratory**. *Further information is contained in a TSP [see page 1].*

NPO-20523

High-Speed Complex-Amplitude Liquid-Crystal SLMs

Frame rates of the order of several kilohertz are achievable.

Lyndon B. Johnson Space Center, Houston, Texas

High-speed complex-amplitude spatial light modulators (SLMs) containing liquid crystals with pixel electronic circuitry on single-crystal-silicon backplanes are undergoing development. The basic approach taken in this project is to use fast-switching liquid-crystal materials and modulation-enhancing device geometries that have not been used in prior display systems.

The modulator materials selected for this project are chiral smectic liquid-crystal (CSLC) materials of the high-tilt type. These materials are capable of modulating light with switching times <100 μs; however, they have traditionally been dismissed with respect to use in analog complex-amplitude SLMs because they give rise to the following disadvantageous device characteristics:

- Rotative switching (rather than variable retardance) occurs and results in bipolar amplitude modulation in the typical crossed-polarizer arrangement. A variable-birefringence device produces coupled phase and amplitude modulation when operated in the same fashion.
- Depths of modulation are inadequate; CSLC materials act to produce either continuous operation over small ranges or else two-state (binary) switching.
- Relatively strong electric fields and thus high drive voltages are needed for full switching in analog CSLCs.

These device characteristics as well as other pertinent issues have been addressed during the project. Accomplishments have included the following:

- Alignment techniques and drive schemes for high-tilt materials to obtain true gray-scale modulation were developed. These CSLC materials directly provide bipolar amplitude modulation (real-axis coverage) and are essential for nondispersive phase modulation.
- A polymer cholesteric liquid crystal has been verified to function as a handedness-preserving mirror, which enhances the modulation depth of a resonated or a two-pass non-resonated phase-only CSLC modulator.
- A nonresonated 2π-radian analog phase modulator containing a cholesteric-liquid-crystal (CLC) mirror and a high-tilt analog half-wave element has been demonstrated.
- A thin-film CLC has been investigated for use as a low-stress planarization layer for a very-large-scale integrated (VLSI)- circuit backplane. The CLC film acts as a phase-flat mirror inasmuch as the top surface is formed against an optical flat. The top surface is reflective and masks the underlying VLSI structures.
- A mathematical-modeling program that utilizes a 4 × 4-matrix technique was developed for use in analyzing the geometries of modulators that exploit rotative switching in CSLCs or variable retardance in nematic liquid crystals.
- Closed-form solutions were derived for the modulators for general input polarizations, giving a variety of available operating curves not obtainable when using nematic liquid crystals. This analysis per-

tains to the arrangement of a reflection-mode SLM with a polarizing beam splitter as an analyzer and beam-routing device.

- The use of a high-voltage backplane was found to improve optical-correlation performance.
- A high-performance 128 × 128 analog SLM with a VLSI backplane was demonstrated (at the time of reporting the information for this article, there were plans to develop subsequent devices with higher pixel densities). This VLSI backplane operates at a potential of 12 volts and at a load rate of 10,000 frames/second, with full analog signal storage at each pixel and a pixel pitch of 40 μm. This VLSI backplane supports a variety of liquid-crystal modulators in addition to those based on high-tilt CSLCs.
- SLM drive circuitry and control software were developed and tested. The SLM drive system is controlled by a personal computer.
- A postprocessing technique for planarizing a VLSI backplane was investigated. The technique involves deposition of a thick oxide layer on the VLSI silicon wafer, followed by chemical-mechanical polishing. After polishing, optical-quality pixels are deposited and connected to the underlying VLSI circuits.

Overall, the project has been instrumental in increasing understanding of the principles of operation and of manufacturing liquid-crystal-on-silicon SLM products.

This work was done by Gary Sharp and Steve Serati of Boulder Nonlinear Systems, Inc., for **Johnson Space Center**. *Further information is contained in a TSP [see page 1].*

MSC-22840

Electronic Systems

Hardware, Techniques, and Processes

13 Electrobiotic Toxic-Agent Sensors

BLANK PAGE

Electrobiotic Toxic-Agent Sensors

Inexpensive, compact, reliable sensors would be easy to use.

NASA's Jet Propulsion Laboratory, Pasadena, California

Electrobiotic sensors have been proposed for detecting toxic substances in a variety of environments. Electrobiotic sensors would be inexpensive, compact units that would be easy to use and could be deployed either singly or in large numbers, depending on the size of an environment to be monitored and/or the need to locate a toxic source within a larger area. For example, multiple electrobiotic sensors might be deployed on a battlefield or at a large-scale mining operation, whereas a single electrobiotic sensor might be used to monitor the air in a laboratory or at an assembly bench where toxic chemicals are used.

The term "electrobiotic" was chosen for these sensors because the front line of sensitivity would be biological entities and the responses of these entities to toxic substances would be sensed and processed by electronic circuitry. More specifically, a typical electrobiotic sensor (see figure) would include very small live nematodes in a suitable medium deposited on an active-pixel sensor (APS) [a state-of-the-art single-chip integrated-circuit array of photodetectors and active readout circuitry]. The movements of the nematodes, which are mutatable to be agent-specific, would be detected through differencing between prompt and delayed pixel readout signals.

A control application-specific integrated circuit (ASIC) on a single chip would monitor the pixel-differencing output of the APS chip to detect movement. If movement were detected, no further action would be taken. If movement were not detected, the control ASIC would activate a microfluidic injection of nicotine to stimulate activity of the nematodes. If activity were still not detected, the nematodes would be assumed to be dead, implicating a toxic environment. The ASIC would then activate the radio transmission of a simple binary signal containing encrypted data on the location of the sensor as determined by a Global Positioning System (GPS) receiver that would also be part of the sensor. If multiple electrobiotic sensors were dispersed over a large area, then they could communicate with each other to relay their status and location data to a central receiver/repeater unit, which would be placed in the area during dispersal of the sensors.

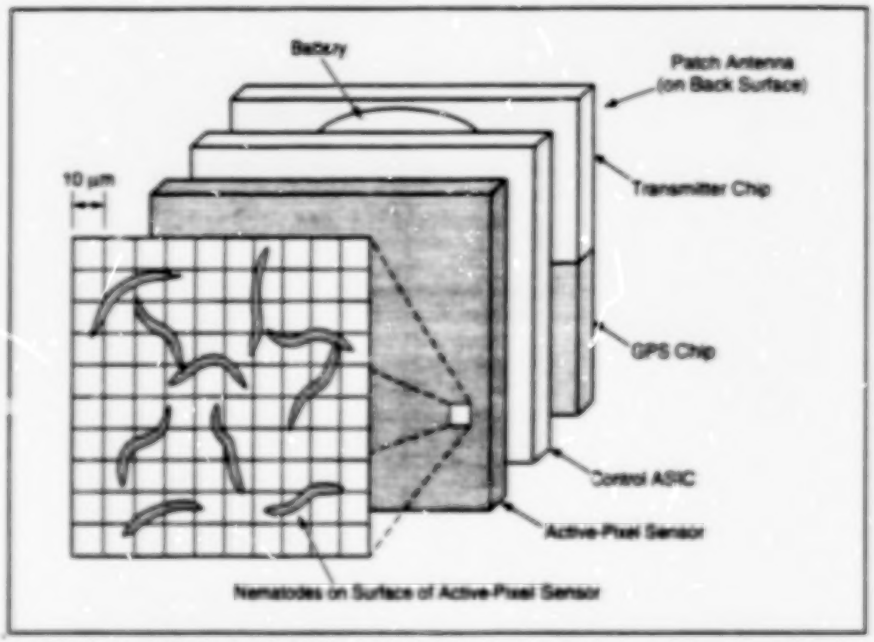

An Electrobiotic Toxic-Agent Sensor would contain and monitor a population of small nematodes. Electronic circuitry would detect motion or lack of motion of the nematodes. Upon detecting cessation of the motion (presumably a result of environmental toxicity), the circuitry would transmit a signal. The total volume of the sensor would be about 1 in.^{3} (~16 cm^3).

The radio transmitter in an electrobiotic sensor could be very simple and short-lived and its range could be limited [e.g., of the order of a mile (~1.6 km)]. Therefore, the power demand of the sensor could be satisfied with a very small battery like that used in a hearing aid.

The life cycles of nematodes are typically of the order of 4 days. However, nematodes can be sustained in a dormant state for a few weeks to a few months. Furthermore, they can be frozen for very long periods. Hence, electrobiotic sensors could be stored at low temperatures for future use.

This work was done by Philip Moynihan, Robert Stirbl, and Roger Kern of Caltech for **NASA's Jet Propulsion Laboratory**. *Further information is contained in a TSP [see page 1].*

NPO-20721

BLANK PAGE

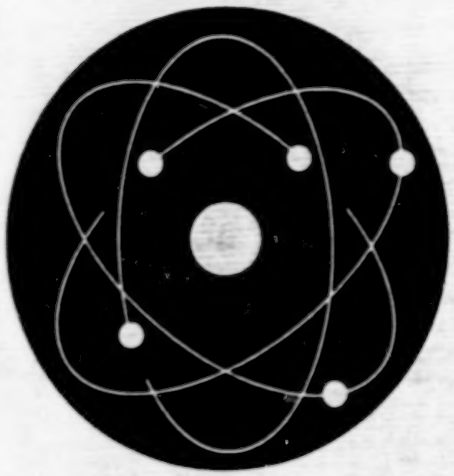

Physical Sciences

Hardware, Techniques, and Processes

17 Tridirectional Gratings as Improved Couplers for QWIPs
18 "Set and Hold With Power Off" Cryogenic Actuators
19 Simplified Radiometer for Quantifying Aircraft Icing Hazard
20 Three-Color Focal-Plane Array of Infrared QWIPs
21 Instrument Measures Fluorescence From Chlorophyll in Plants
22 Two-Color Random Reflectors for QWIPs
24 Dither Sensing for Controlling a Segmented-Mirror Telescope
24 Optical Filters Based on Dense Arrays of Microscopic Pillars
25 Software for Predicting Behavior of a Pyrotechnic Actuator
25 Laser Heating for Testing Rocket-Engine Insulating Phenolic

BLANK PAGE

Tridirectional Gratings as Improved Couplers for QWIPs

Degrees of coupling should exceed those of bidirectional gratings.

NASA's Jet Propulsion Laboratory, Pasadena, California

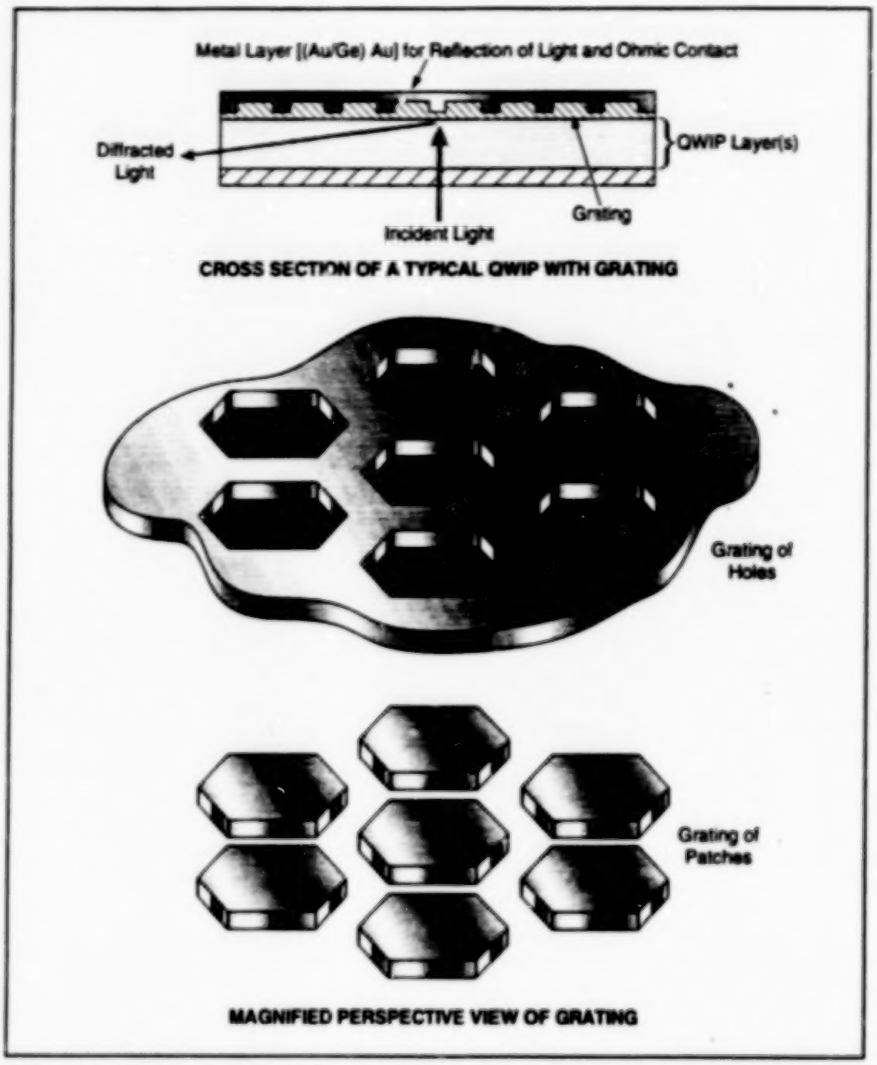
Metal Layer [(Au/Ge) Au] for Reflection of Light and Ohmic Contact
Diffracted Light
QWIP Layer(s)
Grating
Incident Light
CROSS SECTION OF A TYPICAL QWIP WITH GRATING
Grating of Holes
Grating of Patches
MAGNIFIED PERSPECTIVE VIEW OF GRATING

A Hexagonal Pattern of either patches of metal film or holes in an otherwise continuous metal film would constitute a tridirectional grating for coupling of light into the quantum-well layer(s) of a QWIP. The grating would be formed in the cap layer of the QWIP.

Tridirectional diffraction gratings have been proposed to provide optical coupling to quantum-well infrared photodetectors (QWIPs) in focal-plane arrays. The tridirectional gratings would be improved versions of the bidirectional (rectangular-pattern) gratings described in "Cross-Grating Coupling for Focal-Plane Arrays of QWIPS" (NPO-19657), *NASA Tech Briefs*, Vol. 22, No. 1 (January 1998), page 6a. The tridirectional gratings would comprise metal patches or holes arranged in a pattern of closely packed regular hexagonal cells (see figure), with dimensions chosen to optimize diffraction patterns to maximize coupling within narrow spectral bands of interest.

A brief review of the problem of coupling light into a QWIP is prerequisite to an explanation of the improvement expected to accrue from the use of the tridirectional gratings. The QWIP light-coupling problem results from three considerations: (1) the direction through the thicknesses of the quantum wells is perpendicular to the focal plane; (2) quantum selection rules allow the detection of only that part of the incident light that is electrically polarized along the direction through the thicknesses of the quantum wells and thus perpendicular to the focal plane; and (3) the light to be detected is incident along directions approximately perpendicular to the focal plane, and thus only a small fraction of it is electrically polarized along the thicknesses of the quantum wells.

By diffracting light so that at least some of it propagates within the quantum wells at angles other than perpendicular to the focal plane, one changes the plane of polarization so that the through-the-thickness component of polarization is increased. Thus, coupling is increased. The problem in designing a grating (whether linear, bidirectional, or tridirectional) for coupling is to choose the dimensions of the grating to maximize the first-order diffraction of optical power to suitable angles away from the perpendicular. Because a tridirectional grating would exhibit the same periodicity along three directions in the focal plane (instead of only two directions for a corresponding rectangular-pattern cross grating or one direction for a corresponding linear grating), the tridirectional grating would diffract more light to higher angles and thus give rise to increased coupling.

One might be tempted to extend the tridirectional-grating concept to gratings with octagonal or even more complex unit cells in the hope of exploiting periodicity along a greater number of directions. However, this approach would be unlikely to yield any improvement because of a fundamental geometric limitation: Any packing of regular octagons or regular higher polygons in a regular pattern would necessarily create empty interstitial areas.

This work was done by Sumith V. Bandara, Sarath Gunapala, Daniel Wilson, and John K. Liu of Caltech for **NASA's Jet Propulsion Laboratory**. ***Further information is contained in a TSP [see page 1].***

In accordance with Public Law 96-517, the contractor has elected to retain title to this invention. Inquiries concerning rights for its commercial use should be addressed to

Technology Reporting Office
JPL
Mail Stop 122-116
4800 Oak Grove Drive
Pasadena, CA 91109
(818) 354-2240

Refer to NPO-20703, volume and number of this NASA Tech Briefs *issue, and the page number.*

"Set and Hold With Power Off" Cryogenic Actuators

Magnetic fields would be applied to magnetostrictive rods by high-temperature-superconductor electromagnets.

Langley Research Center, Hampton, Virginia

Magnetostrictive actuators that would hold their displacements with power turned off have been proposed for use at temperatures from about 10 to about 77 K. Such "set and hold with power off" actuators are attractive for effecting fine position adjustments in cryogenic scientific instruments, wherein significant amounts of heat would be released and could disturb instrument operation if it were necessary to apply power continually to maintain actuator displacements.

The essential components of a magnetostrictive actuator are a rod of magnetostrictive material and an electromagnet coil to control the magnetic field applied to the rod. In an actuator of the proposed type, the magnetostrictive material would be single-crystal $Tb_{0.6}Dy_{0.4}Zn$, which exhibits a saturation magnetostrictive strain of as much as 0.5 percent at a preload stress of only 13.8 MPa and an applied magnetic field of about 500 Oersted ($\approx 4 \times 10^4$ A/m). The magnetostrictive rod would be surrounded by an electromagnet coil in the form of a monolithic cylinder made of a high-temperature superconductor (see Figure 1), which could be either $YBa_2Cu_3O_{7-x}$ or $Bi_2Sr_2CaCu_2O_{8+\delta}$ (aka BSCCO 2212). The persistent magnetic field needed to maintain a constant magnetostrictive stain (in order to hold a constant displacement with power off) would be generated by an electrical current flowing circumferentially in the superconductive cylinder.

The superconductive cylinder would be charged with the desired current by applying a suitable pulsed current to a normally conductive (e.g., copper-wire) solenoidal electromagnet coil surrounding the superconductive cylinder. The pulse would be tailored so that, at first, the superconductor would first be brought to its critical state (which occurs at the maximum superconducting current), and then additional magnetic field would be applied, all at nearly constant temperature. In the critical state, magnetic flux could be made to move freely into or out of the cylinder (flux could be pumped) with some attendant dissipation that would cause a momentary small increase in temperature. The increase in temperature would be too small to disrupt the superconductivity.

A circuit to implement this charging scheme is depicted in Figure 2, wherein the normally conductive charging coil is represented by inductor L1, the superconductive cylinder is represented by inductor L2. The momentarily dissipative nature of the superconductive cylinder is represented by resistor R, which limits the current in L2 to no more than the critical current, and which is zero when the current in L2 is smaller than the critical current.

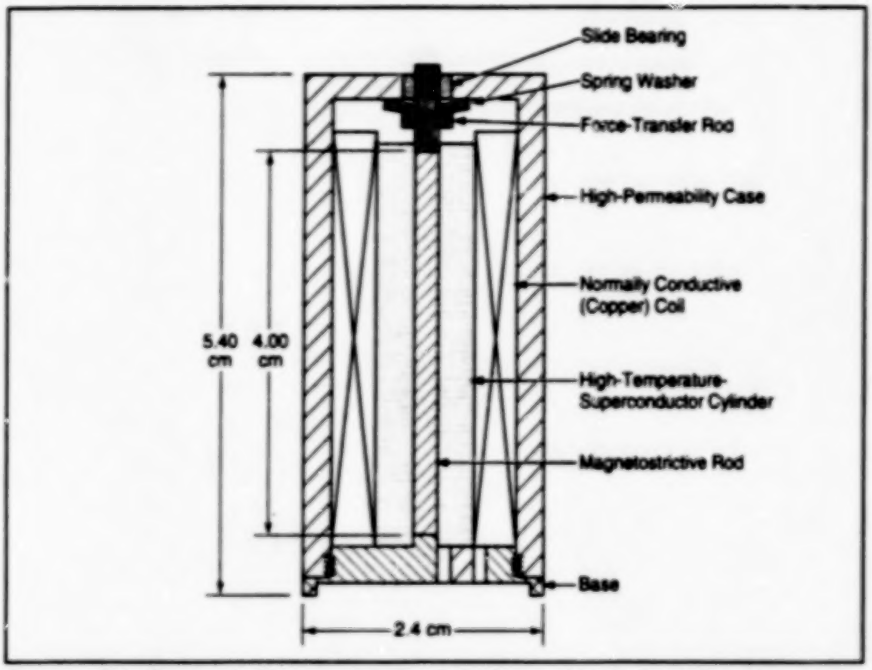

Figure 1. This Cryogenic Magnetostrictive Actuator would hold its position when power was not applied, by virtue of the persistent current flowing circumferentially in the high-temperature-superconductor cylinder.

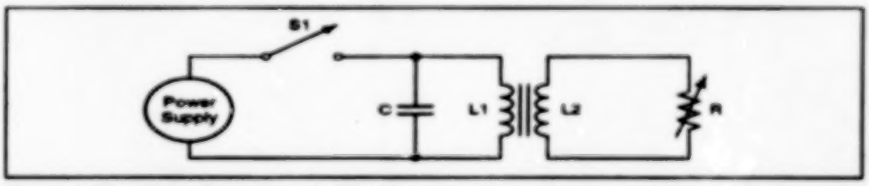

Figure 2. This Pulse/Transformer Circuit would charge the superconductive cylinder to the current needed to maintain the desired actuator displacement.

In preparation for generating a pulse of charging current, switch S1 would be closed to charge the capacitor from the power supply. Once the capacitor was charged, switch S1 would be opened and switch S2 would be closed. Assuming a high coefficient of coupling between L1 and L2, the current in L1 would rise rapidly immediately following closure of S2 because, at that time, the combination of L1 and L2 would constitute a transformer with a short-circuited secondary winding. The increase in current in L1 would be balanced by an opposite change in the current in L2. Once the current in L2 reached the critical value, it would remain steady at that value and the load presented to the capacitor would suddenly become inductive, slowing down the rate of increase of current in L1. The circuit would then behave like an ordinary capacitor-and-inductor system with a characteristic oscillation period.

Once the current in L1 reached its maximum value and started to decay, the state of the superconductor would depart from criticality; therefore, the inductive load would suddenly disappear and the circuit would once again become a short circuit, with no voltage but large current. With no driving voltage, the current in L1 would decay very rapidly, without oscillations. The final result would be that the energy in the capacitor, minus the energy dissipated in L1, would be transferred to the superconductor.

The charging process as described thus far could be repeated until the current in the

superconductive cylinder had increased to the desired value (but not more than the critical value). The current in the superconductive cylinder could also be made to decrease in a discharging process, which would be the identical to the charging process except that the capacitor would be charged in opposite polarity.

This work was done by Garnett C. Horner of **Langley Research Center**, *Leslie Bromberg of Massachusetts Institute of Technology, and J. P. Teter of the Naval Surface Warfare Center. Further information is contained in a TSP [see page 1].*
L-17837

Simplified Radiometer for Quantifying Aircraft Icing Hazard

A single radiometer would supplant a more-complex system that includes two radiometers.

NASA's Jet Propulsion Laboratory, Pasadena, California

A simplified microwave radiometric apparatus has been proposed for use in quantifying the potential danger of accretion of ice onto an aircraft flying through a cloud. The quantity of interest, called the "icing hazard potential" (IHP), is the product of (1) the liquid-water content (LWC) of the cloud at a given altitude and (2) some function of the degree of supercooling of the liquid water at that altitude.

In 1983, it was demonstrated that reliable values of IHP could be calculated from readings of a ground-based instrumentation system that comprised (1) a water-vapor radiometer (for measuring LWC), (2) a microwave temperature profiler (MTP) (to measure the vertical temperature profile), (3) a hand-held infrared radiometer (to measure the cloud-base temperature and thus, in conjunction with the MTP, the cloud-base altitude), and (4) a surface meteorological subsystem (to measure surface values of temperature, barometric pressure, and humidity). The proposed system would share some features in common with the 1983 system, but would not include a water-vapor radiometer. Inasmuch as the radiometers embodied most of the cost the 1983 system, eliminating one radiometer would reduce the cost significantly.

To be able to determine the IHP, one needs to know the temperature and the LWC as a function of altitude. For the purpose of measuring these quantities, the proposed system would exploit the radiometric characteristics of oxygen and liquid water in the frequency range from about 50 to about 70 GHz. The absorption spectrum of oxygen molecules in this frequency range (see figure) depends on temperature, pressure, and water-vapor density. The brightness temperature observed by an MTP is an exponentially weighted average of all oxygen emission along its line of sight and closely approximates the air temperature at an effective distance from the radiometer equal to the reciprocal of the absorption coefficient.

Consider two observation frequencies — one on the high-frequency and one on the low-frequency side of the peak in the oxygen absorption spectrum — for which the absorption coefficient is equal. In the absence of cloud liquid water along the line of sight within the effective distance, the brightness temperatures observed at both frequencies would be the same, but in the presence of cloud liquid water, the brightness temperatures observed at the higher frequency would exceed that observed at the lower frequency, because cloud liquid water contributes to brightness temperature by an amount approximately proportional to the square of frequency. Thus, in principle, one could infer both the air temperature and the LWC from the brightness temperatures at the two frequencies.

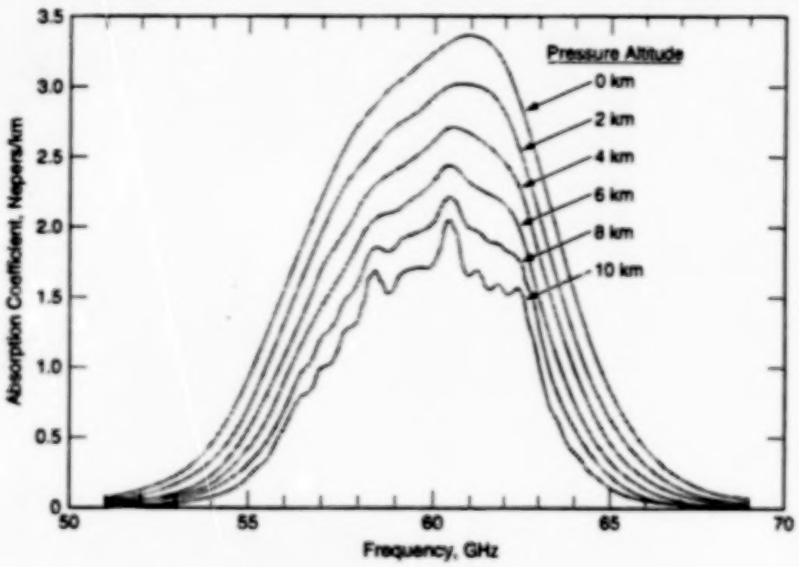

The Absorption Spectrum of Oxygen in the absence of cloud liquid water depends on frequency and pressure altitude; it also depends on temperature and water-vapor density, nominal values of which were assumed in computing these curves.

The main radiometer in the proposed apparatus would be an extended version of an airborne MTP now in use. As such, it would include a scanning mirror used to scan the line of sight in elevation angle while measurements were taken at several pairs of frequencies (and thus several effective distances), the net effect being to acquire data from different effective altitudes. The apparatus would also include an infrared gun operating in the wavelength range of 8 to 14 μm to determine the cloud-base altitude, plus simple sensors to measure the ambient temperature, pressure, and relative humidity.

The proposed apparatus would cost less than airport and aircraft radar systems do. Eventually, taking advantage of monolithic microwave integrated circuitry, it should be possible to mass-produce the apparatus and install it in aircraft at relatively low cost. Because icing is of particular concern during long, slow descents and approaches, prior to miniaturization and mass production, it could be desirable to install copies of the apparatus on the approach paths of major airports to warn approaching aircraft of potential icing hazards.

This work was done by Michael J. Mahoney of Caltech for **NASA's Jet Propulsion Laboratory**. *Further information is contained in a TSP [see page 1].*
NPO-20291

Three-Color Focal-Plane Array of Infrared QWIPs

Three-wavelength imaging would provide enhanced temperature-measurement capability.

NASA's Jet Propulsion Laboratory, Pasadena, California

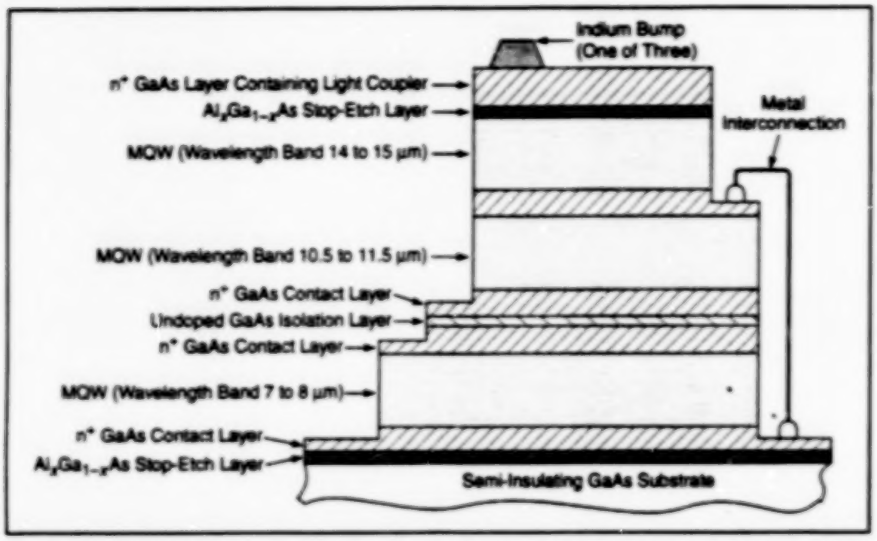

The Device Structure is shown here for only one of many pixels, for the sake of simplicity. Each MQW structure within a pixel would be photosensitive in one of three infrared wavelength bands; thus, the device would sense a three-color infrared image.

A proposed focal-plane array (FPA) of quantum-well infrared photodetectors (QWIPs) would sense images in three different infrared wavelength bands simultaneously. These and other QWIP infrared image sensors are undergoing development for use in measuring temperature distributions in images; potential applications include scientific (e.g., remote sensing of the Earth and other planets) and military (e.g., discriminating between targets and other objects in terms of temperature).

A one-color QWIP FPA can produce data for an absolute-temperature map of the scene only if the emissivities of the objects in the scene are known. A two-color QWIP FPA can produce data for an absolute-temperature map of the scene even when the emissivities are unknown, provided that the sensed radiation consists solely of thermal radiation from the objects in the scene. The proposed three-color QWIP FPA could produce data for a temperature map of the scene even when the sensed radiation from the object included an unknown component of infrared light, reflected from objects in the scene, that originated at an external source.

The proposed device would be fabricated from a wafer that would comprise multiple layers of $Al_xGa_{1-x}As$ formed by molecular-beam epitaxy on a semi-insulating GaAs substrate. Each pixel of the device would contain a stack of three multiple-quantum-well (MQW) $Al_xGa_{1-x}As$ structures. Each MQW structure would be designed for peak photosensitivity in one of the three wavelength bands (see figure): The top MQW structure would be designed for bound-to-bound photoexcitation of electrons in the wavelength band of 14 to 15 μm; the middle MQW structure would be designed for bound-to-quasi-bound excitation in the wavelength band of 10.5 to 11.5 μm; and the bottom MQW structure would be designed for bound-to-continuum excitation in the wavelength band of 7 to 8 μm.

Each MQW structure would consist of approximately 30 periods, each period comprising (1) an $Al_xGa_{1-x}As$ barrier layer 500 Å thick and (2) a GaAs well layer. The mole fraction of aluminum (x) in the barrier layers and the geometric depth of the wells would be chosen to obtain the required spectral response; and the foregoing parameters would be chosen, along with the doping densities and the precise number of periods, to optimize the device for a specific application. The top and middle MQW structures would be separated by a 0.5-μm-thick n+-doped GaAs contact layer. The middle and bottom MQW structures would be separated by a 0.5-μm-thick undoped (and therefore highly electrically resistive) GaAs isolation layer. Two n+-doped GaAs contact layers would be grown on both sides of the isolation layer to serve as independent electrical contacts for the middle and bottom MQW stacks.

The three-color QWIP structure as described thus far would be grown on top of a 0.5-μm-thick n+-doped GaAs bottom contact layer on top of an $Al_xGa_{1-x}As$ etch-stop layer on the GaAs substrate. A 300-Å-thick $Al_{0.3}Ga_{0.7}As$ stop-etch layer would be grown on top of the topmost n+-doped GaAs contact layer. On top of the stop-etch layer, a 1.3-μm-thick n+-doped GaAs contact and cap layer would be grown, and a light coupler would be fabricated in this layer as described subsequently. The contact layer between the top and middle MQW structures would be short-circuited to the contact layer between the bottom MQW and the substrate, to establish a common (ground) bus. Only three indium bumps per pixel would be needed for bonding the device to a silicon readout integrated circuit that would provide independent readout for each wavelength in each pixel.

As explained in more detail in several prior *NASA Tech Briefs* articles, in order to make photoexcitation possible, a light coupler is needed to alter the polarization of normally incident light so that the light propagating within the device is polarized at least partly along the through-the-thickness direction. In the proposed device, the light coupler would be an achromatic array of reflectors comprising a square pattern of cells, each cell comprising a three-by-three array of subcells. Within each cell, the depths of eight subcells would be chosen to obtain destructive interference at the middle wavelengths of all three wavelength bands; the depth of the ninth subcell would be chosen at random. The cell surfaces would be coated with Au/Ge and Au for ohmic contact and reflection.

This work was done by Sumith Bandara, Sarath Gunapala, John K. Liu, Daniel Wilson, and William Parrish of Caltech for **NASA's Jet Propulsion Laboratory**. *Further information is contained in a TSP [see page 1].*

In accordance with Public Law 96-517, the contractor has elected to retain title to this invention. Inquiries concerning rights for its commercial use should be addressed to

Technology Reporting Office
JPL
Mail Stop 122-116
4800 Oak Grove Drive
Pasadena, CA 91109
(818) 354-2240

Refer to NPO-20683, volume and number of this NASA Tech Briefs *issue, and the page number.*

Instrument Measures Fluorescence From Chlorophyll in Plants

Effective discrimination against solar background radiation is achieved without critical optical and mechanical parts.

Stennis Space Center, Mississippi

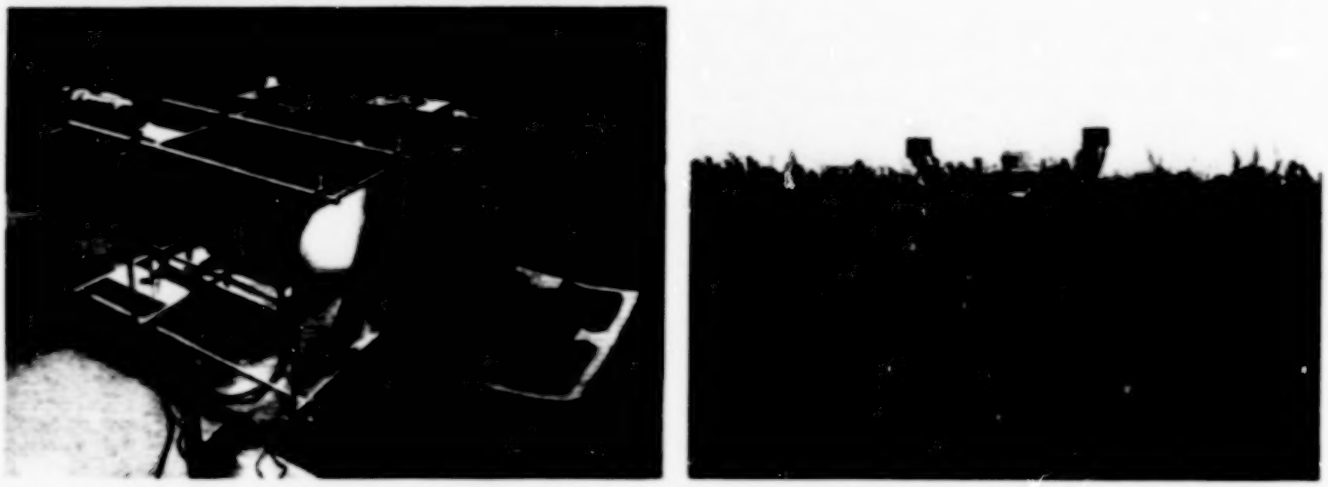

Figure 1. The **Plant Fluorescence Sensor** in the left view is lying, with its casing removed, on a utility cart. In the right view, it is installed on a high-clearance vehicle for monitoring a Nebraska corn field.

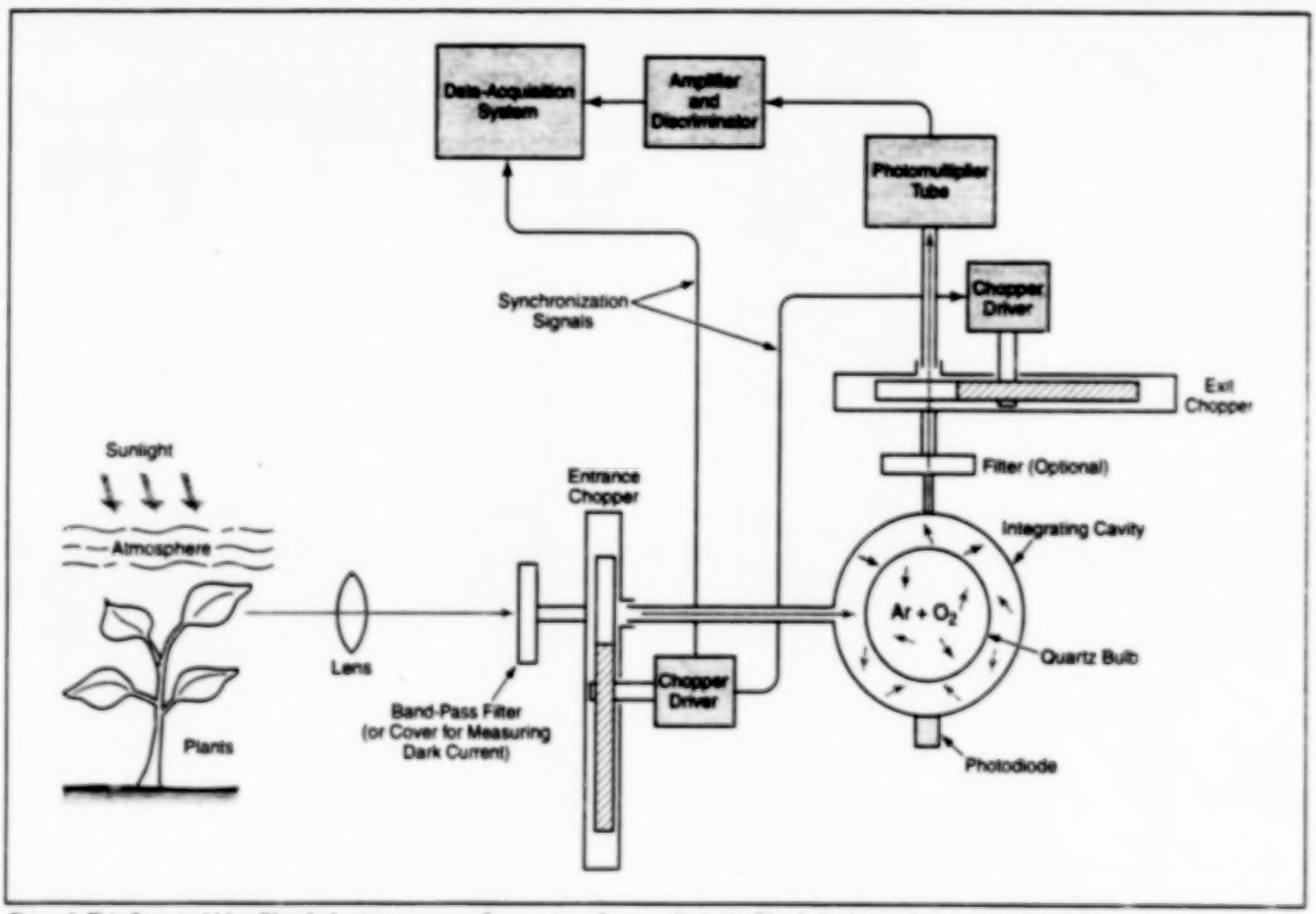

Figure 2. This **Spectral-Line Discriminator** measures fluorescence from sunlit plants. Discrimination against scattered sunlight is achieved by a design that utilizes the absorption spectrum of atmospheric oxygen in combination with absorption and fluorescence in a bulb that contains oxygen.

An optoelectronic instrument, known as a plant fluorescence sensor, is being developed for use as a working tool in agricultural settings. This instrument is a remote, passive monitor that provides a means of discerning plant stress at very early stages. With sufficient warning, the user could provide timely applications of fertilizer, water, and/or pesticide to achieve maximum crop yield at minimum cost. Figure 1 presents two views of the plant fluorescence sensor. The instrument is the subject of U. S. Patent 5,567,947.

Measurement of steady-state plant fluorescence offers the possibility of determin-

ing the physiological status of a green plant. The magnitude of plant fluorescence and its spectral (color) distribution is sensitive to a number of factors which are related to the ability of a plant to perform photosynthesis (the process by which green plants convert atmospheric water vapor and carbon dioxide into sugars and oxygen, using sunlight as fuel). For instance, the light capture efficiency of the plant is dependent on the type and amount of pigment molecules (such as chlorophyll) which in turn is dependent on adequate fertilization. Plants stressed from a lack of fertilizer will limit chlorophyll production and exhibit both lower overall level of fluorescence and shift in spectral distribution compared to healthy plants. Another factor, such as lack of adequate water, can serve to limit the rate of photosynthesis by causing the plant to close its stomata (the openings which allow the leaf to draw in carbon dioxide and water vapor); when this happens, the level of plant fluorescence will generally increase. Thus, measurements taken with this sensor can guide growers in the allocation of resources such as irrigation water, fertilizer, and pesticides.

Under sunlight, the chlorophyll in plants fluoresces at wavelengths from about 660 to 800 nm. The major problem in measuring this fluorescence is to discriminate against scattered sunlight, which can contribute a spurious component to the measurement. The present sensor is of the class of apparatuses known as Fraunhofer-line or spectral-line discriminators, but this sensor differs from others of its class by virtue of a unique design that exploits the spectral absorption lines of oxygen in such a way as to obtain enhanced spectral discrimination at lower cost. The desired spectral resolution and discrimination are achieved without need for the highly precise, expensive optical components with critical mechanical adjustments (e.g., Fabry-Perot cavities) that are used in other spectral-line discriminators.

Atmospheric oxygen strongly attenuates incident sunlight in spectral lines in two groups known as A band (wavelength ≈760 nm) and B band (wavelength ≈688 nm). Each of these bands includes about 40 spectral lines with such strong absorption that the atmosphere can be considered opaque at the middle wavelengths of these lines. Chlorophyll fluoresces strongly at these wavelengths. Thus, if light from plants at these wavelengths is measured, one can be assured that the measurement represents only fluorescence from chlorophyll, without contribution from scattered sunlight. Of course, the measuring instrument must be close enough to the plants in question that atmospheric oxygen does not also appreciably absorb the fluorescence from the chlorophyll, along with sunlight at the affected wavelengths: the resulting practical limit on the range of the present instrument or any similar instrument is 100 to 200 meters.

The present sensor (see Figure 2) is based on this spectral-discrimination principle. Light from sunlit plants is focused by a lens, then made to pass through a filter that passes wavelengths in a chosen 10-nm-wide subband of A or B band. The band-pass-filtered light passes through an entrance chopper, then along a light pipe to a spherical integrating cavity. Centered in the cavity is a quartz bulb that contains a gaseous mixture of oxygen and argon at a total pressure of about 100 torr (about 13 kPa).

When the entrance-chopper aperture is open, the oxygen in the bulb is illuminated by plant fluorescence plus scattered sunlight in the chosen subband of A or B band, but the oxygen absorbs only the light at its characteristic absorption wavelength in this subband. Because the atmosphere has already filtered out sunlight at these wavelengths, the light absorbed by the oxygen consists almost entirely of fluorescence emitted by the plants. While the entrance-chopper aperture remains open, a silicon photodiode measures the total A- or B-band radiation received by the cavity.

When the entrance-chopper aperture is closed, the oxygen in the bulb emits the absorbed light energy as fluorescence in A band (regardless of whether the illumination is in A band or B band). Because the entrance-chopper aperture is closed, the remaining light in the cavity consists entirely of this secondary fluorescence, proportional to the fluorescence from the plants. An exit chopper synchronized in opposite phase with the entrance chopper opens to allow this light to pass to a photomultiplier tube cooled to a temperature 40 K below ambient. The output of the photomultiplier tube is processed and fed to a data-acquisition system.

This work was completed by Paul L. Kebabian, Herman E. Scott, and Andrew Freedman of Aerodyne Research, Inc., for **Stennis Space Center** *under 1996 SBIR Phase II: NAS #NAS13-707. For further information, contact Herman Scott of Aerodyne Research, Inc., at (978) 663-9500 extension 267.*

In accordance with Public Law 96-517, the contractor has elected to retain title to this invention. Inquiries concerning rights for its commercial use should be addressed to

Laurie S. Dean, Commercialization Manager
Aerodyne Research, Inc.
45 Manning Road
Billerica, MA 01821-3976

Refer to SSC-00037, volume and number of this NASA Tech Briefs *issue, and the page number.*

Two-Color Random Reflectors for QWIPs

Reflectors could be designed for two-band or single-broad-band response.

NASA's Jet Propulsion Laboratory, Pasadena, California

Random reflectors of a proposed type would be fabricated on the back surfaces of quantum-well infrared photodetectors (QWIPs) to increase the coupling efficiency of infrared light into the QWIPs in two wavelength bands. A reflective surface according to this proposal would comprise an array of square cells, each cell divided into a 2-by-2 array of subcells that would lie at various, partly random depths relative to the nominal flat back surface of the QWIP. The subcells at the various depths would be formed by one of several lithographic processes, depending on the specific design. In comparison with the light-scattering efficiency of crossed-diffraction-grating QWIP light couplers that have been reported previously in *NASA Tech Briefs*, the light-scattering efficiency of the proposed random reflectors would be less dependent on wavelength; this would be an advantage in QWIP applications in which there are requirements for broad-band or multiband response.

As discussed in more detail in several prior articles in *NASA Tech Briefs*, in order to couple light into a QWIP, the quantum-well layers of which lie parallel to its focal plane, it is necessary to cause light to propagate within the QWIP along a direction other than perpendicular to the focal plane; the efficiency of coupling increases with the angle between the direction of propagation and the perpendicular. Most of the incoming light is concentrated within a small angular range about the perpendicular. Therefore, the pur-

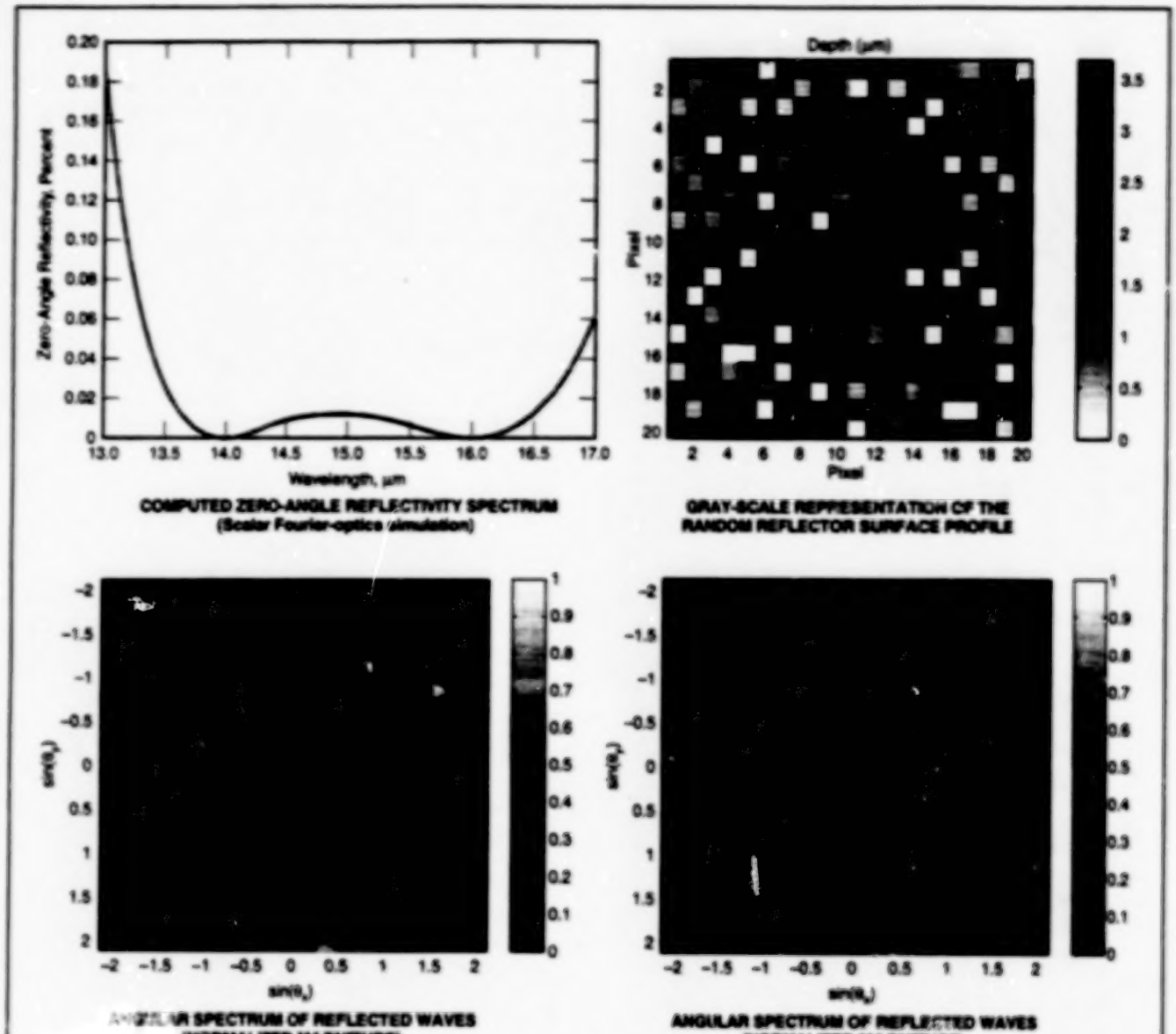

The Zero-Angle Reflectivity Spectrum and the Diffraction Pattern were computed for the reflector pattern shown at the top. (The actual reflectivity would probably be greater but similar in shape.) The computations were based on free-space wavelengths of 14 and 16 μm, a subcell (reflector-grid) interval of 2.5 μm, and an index of refraction of QWIP material of 3.1. A free-space wavelength of 15 μm was used in calculating the diffraction pattern.

pose served by the proposed random reflectors and by the previously reported cross-grating QWIP light couplers is to exploit diffraction to divert the incoming light, as efficiently as possible, to propagation at large angles from the perpendicular. Additionally, light that is not absorbed will get reflected and encounter a different structure on each bounce. This improves the ability of the QWIP to trap the light and absorb a larger fraction of photons.

For maximum diffraction at high angles, the subcells would be given dimensions of the order of the wavelengths of interest. It would also be necessary to minimize low-angle diffraction in order to minimize waste of light. Therefore, the depths of the subcells would be chosen so that at the middle wavelengths of both wavelength bands of interest, any light propagating along the perpendicular direction would interfere destructively. Specifically, the depths of the four subcells (d_i, i = 1 to 4) of a given cell would be as follows:

d_1 = a random value between 0 and $\lambda_1/4$,
$d_2 = d_1 + \lambda_1/4$,
$d_3 = d_1 + \lambda_2/4$, and
$d_4 = d_1 + \lambda_1/4 + \lambda_2/4$,

where λ_1 and λ_2 are the two wavelengths of interest inside the QWIP material.

This choice of depths would cause the subcells to act in pairs to produce destructive interference: At λ_1, destructive interference would occur between subcells 1 and 2 and between subcells 3 and 4; at λ_2, destructive interference would occur between subcells 1 and 3 and between subcells 2 and 4.

The figure shows a gray-scale representation of a reflector pattern of this type, a plot of the computed zero-angle (perpendicular) reflectivity, and a gray-scale representation of the computed diffraction magnitude as a function of the sine of the angular deviation (θ) from the perpendicular. All waves inside the circle of radius $\sin(\theta) = 1$ are propagating, and those outside the circle are evanescent. As needed for efficient coupling, the computed zero-angle reflectivity goes to zero at the two design wavelengths and the computed diffraction magnitude at high angles is strong.

This work was done by Daniel Wilson,

Sumith Bandara, Sarath Gunapala, and John K. Liu of Caltech for **NASA's Jet Propulsion Laboratory**. *Further information is contained in a TSP [see page 1].*

In accordance with Public Law 96-517, the contractor has elected to retain title to this invention. Inquiries concerning rights for its commercial use should be addressed to

Technology Reporting Office
JPL
Mail Stop 122-116
4800 Oak Grove Drive
Pasadena, CA 91109
(818) 354-2240

Refer to NPO-20682, volume and number of this NASA Tech Briefs issue, and the page number.

Dither Sensing for Controlling a Segmented-Mirror Telescope

Images of distant point sources are processed to obtain wavefront-correction control signals.

Marshall Space Flight Center, Alabama

Image-plane multidither sensing has been found to be suitable for adaptive wavefront correction in a large telescope in which the main optic is a precise reflector divided into lightweight, controllably actuated segments. In image-plane multidither sensing, the telescope is aimed at a star or other distant point source and image data are recorded as each segment in turn is dithered slightly about a nominal position and orientation. The image data are processed into actuator-control signals for adjusting the nominal segment positions and orientations to obtain the desired wavefront correction.

For this method to be effective, the telescope system must be quasi-static in the sense that any mechanical and optical disturbances in the system must be characterized by times appreciably longer than the time needed to complete the corrective cycle of dithers and measurements, processing of measurement data, and controlled actuation. The position and orientation errors of each segment, and the corresponding translational and rotational displacements needed to effect correction, are called "piston" (simple translation along the line of sight) and "tilt" (angular displacements about two axes perpendicular to the line of sight). The tilt-correction procedure is based on geometric optics and can be performed at any time. However, the piston-correction procedure is based partly on phase coherence; therefore, in practice, the tilt correction must be made first to provide the coherence needed for the piston correction.

In the tilt-correction procedure, a segment is dithered in tilt and initial and final images are recorded. Although the image plane can be cluttered with subimages from multiple segments, the subimages of all other segments can be suppressed and the displacement of the segment in question tracked by subtracting the initial image from the final image and finding the centroid of the difference image. Subtraction and centroiding are common operations in image processing, and circuit boards that perform these operations are commercially available.

The angular displacement of the dither should be at least twice the diffractive size (wavelength ÷ aperture width) of a segment to enable clear differentiation of the initial and final images. Once the centroid has been located, the segment of interest is tilted to move the subimage cast by that segment to the desired location, which is ordinarily the center of the image plane. This procedure is repeated for each segment in turn, until all have been thus corrected in tilt.

In comparison with tilt corrections, piston corrections are more difficult. The piston measurement for each segment is a measurement of the response of the speckle pattern to a small dither of that segment. There are several alternative piston-correction procedures, each based on a different combination of (1) a quantitative measure of the speckle pattern and (2) determining the signs and magnitudes of piston displacements needed to correct the speckle pattern according to the quantitative measure.

To the extent to which the piston-correction procedures are based on phase coherence, they are subject to the integer-multiple-of-2π-radians phase ambiguity at a given wavelength. Measurements can be performed at multiple wavelengths to resolve this ambiguity; alternatively, one could use broadband light from a stellar source, although this can entail complications at large displacements. The use of less-accurate electronic or mechanical edge sensors might be a more-practical solution.

This work was done by Glenn W. Zeiders of The Sirius Group for **Marshall Space Flight Center**. *For further information, contact the Sirius Group at gzeiders@prodigy.net.*

Inquiries concerning rights for the commercial use of this invention should be addressed to the Patent Counsel, Marshall Space Flight Center [see page 1]. Refer to MFS-31352.

Optical Filters Based on Dense Arrays of Microscopic Pillars

Structures found in moth eyes would be adapted to a variety of uses.

NASA's Jet Propulsion Laboratory, Pasadena, California

A proposal for development of a class of high-transmission and antireflection optical filters is derived from the observation that the eyes of moths reflect almost no light, regardless of the wavelength or the angle of incidence of illumination. The low-reflection property of moth eyes is attributable to dense arrays of microscopic pillars that exhibit little or no diffraction or scattering. This is because (1) the dimensions and pitches of the pillars are smaller than the shortest wavelength of incident light in the wavelength range of interest and (2) a dense array of pillars provides a gradual transition in density from open space to a bulk solid material, so that an abrupt density change, which would generate reflections, is not present.

Long-wavelength-pass filters based on this principle could be used in spectrometers and possibly other optical instruments. For example, one could build a matrix of arrays of microscopic pillars over a matrix of miniature thermoelectric devices, thermopiles, or other detectors. The pillars in each array would have a size and pitch corresponding to a specific cutoff wavelength. Each array would transmit (almost totally) only light at wavelengths greater than its cutoff wavelength to the underlying detectors. The multiplicity of cutoff wavelengths associated with the arrays in the matrix would define increments of a spectrum; thus, in effect, one would have a filter/sensor spectrometer unit - with no moving parts.

Large surfaces textured with moth-eye textures have been fabricated by use of holography. To fabricate arrays of microscopic pillars with specific sizes and shapes (or to fabricate matrices of such arrays with different pitches for different cutoff wavelengths), it would be necessary to use x-ray lithography. For example, one would expose a negative x-ray resist to x-rays through a density mask containing nanometer-scale features created by electron-beam milling. The pillars would then be formed as the material left after etching of the exposed resist.

It has also been proposed to make variable-cutoff long-wavelength-pass filters. Such a filter would consist of an array of suitably shaped, sized, and pitched micropillars on a transparent piezoelectric substrate. The cutoff wavelength would be varied by applying a voltage to expand or contract the substrate.

This work was done by Frank Hartley of Caltech for **NASA's Jet Propulsion Laboratory**. *Further information is contained in a TSP [see page 1].*
NPO-20448

Software for Predicting Behavior of a Pyrotechnic Actuator

This software has remedied conceptual errors in some prior design models.

John H. Glenn Research Center, Cleveland, Ohio

A theoretical model that predicts the time-dependent behavior of a pyrotechnically actuated mechanism and a computer program that implements the model have been developed. The model and program are especially applicable to a pyrotechnic device known as the NASA Standard Initiator (NSI). Before this model and program were developed, the only principles that guided the design of pyrotechnically actuated mechanisms were those derived through empiricism.

The theoretical model includes (1) equations of conservation of mass, momentum, and energy, (2) equations of state, (3) equations of reaction kinetics, and (4) the assumption that there are no spatial variations in the relevant physical and chemical quantities (the "well stirred reactor" assumption). The computer program that solves the model equations is written in FORTRAN 77. This program requires the use of two other programs, known as "CET88" and "Chemkin," that are standard for calculations of the type in question.

The program has been found to predict accurately (as determined by comparison with experimental observations) the pressure history of an NSI firing into a pin-puller device, a closed vessel that has a volume of 10 cm^3, and an apparatus called the "Dynamic Test Device." The program has also remedied several conceptual errors in prior design models.

This work was done by Joseph M. Powers and Keith A. Gonthier of the University of Notre Dame for **Glenn Research Center**. *Further information is contained in a TSP [see page 1].*

Inquiries concerning rights for the commercial use of this invention should be addressed to NASA Glenn Research Center, Commercial Technology Office, Attn: Steve Fedor, Mail Stop 4–8, 21000 Brookpark Road, Cleveland, Ohio 44135. Refer to LEW-16869.

Laser Heating for Testing Rocket-Engine Insulating Phenolic

A continuous-wave CO_2 laser has been selected as a source of heat for testing the thermal response of carbon-cloth phenolic like that used as insulating material in a reusable solid-fuel rocket motor (RSRM). The particular thermal response of interest, observed during operation of an RSRM, is pocketing. By suitable adjustment of the size and power of the laser beam, the rate of heating can be made nearly identical to that in the RSRM nozzle during operation.

The use of the laser as the source of heat in such testing is accompanied by the use of optical means to measure the surface temperatures of specimens. The surface-temperature measurements make it possible to construct better mathematical models and develop better understanding of the thermal response of the material under test. Moreover, unlike the environment in a test motor during operation, the environment in the vicinity of a laser-heated specimen is not dominated by hot chemicals in high concentrations; as a result, additional instrumentation that cannot be used in tests in an operating rocket engine can be used in laser-heating tests.

This work was done by Timothy N. Johnson and Edward C. Mathias of Thiokol Corp. for **Marshall Space Flight Center**.
MFS-31272

BLANK PAGE

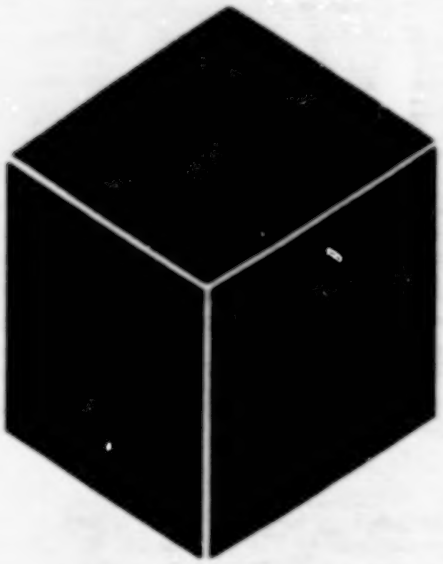

Materials

Hardware, Techniques, and Processes

29 RTM-Processable Resins Containing Thermosetting Plasticizers
30 Burn-Resistant, Strong Nickel Alloys
31 Self-Temperature-Compensated Ceramic Strain Gauges
31 Aurogels With Gradients of Density
31 Molded Plastic Simulated Landscapes

BLANK PAGE

RTM-Processable Resins Containing Thermosetting Plasticizers

These plasticizers lower viscosities without giving rise to volatiles.

John H. Glenn Research Center, Cleveland, Ohio

A number of matrix resins that contain thermosetting plasticizers have been developed for use in the resin-transfer molding (RTM) of composite-material (fiber/matrix) parts. These resins and composites are candidates for use in manufacturing lightweight components of aircraft engines and other structures that must withstand temperatures up to and perhaps somewhat above 300 °C.

RTM is attractive for this purpose because it is a relatively inexpensive process for producing medium quantities (typically, thousands) of complexly shaped parts. In RTM, a fiber preform is infiltrated with a molten resin that, typically, has been partially pre-cured ("staged"). For making high-quality parts, a resin to be used in RTM must have the following characteristics:

- Its viscosity must be low enough to allow it to flow through the preform without distorting the preform;
- It must wet the fibers adequately;
- Its pot life at the RTM processing temperature and viscosity must be at least 30 minutes; and
- It must outgas as little as possible during filling of the mold and subsequent curing of the resin.

The present resins are based on the AMB-21 resin system — a less-toxic system recently developed as an alternative to the PMR-15 polyimide system. [The industry standard polyimide matrix resin, PMR-15 was developed at Lewis Research Center (since named Glenn Research Center) in 1971. The PMR-15 monomer mixture includes methylenedianiline (MDA), a suspected carcinogen.] The basic AMB-21 prepolymer solution is a made by combining three monomeric solutions:

- 3,3',4,4'-benzophenonetetra-carboxylic ester (BTDE) in methanol;
- the monomethyl ester of norbornene-2,3-dicarboxylic acid (NE) in methanol; and
- bis(aminophenoxy) propane (BAPP) in tetrahydrofuran (THF), acetone, or toluene.

The basic AMB-21 prepolymer does not have the correct rheological properties for RTM; in particular, its viscosity is too high. The approach taken in the development of the present resins involved the reduction of viscosity through the addition of thermosetting plasticizers (more specifically, low-viscosity reactive diluents that are chemically compatible with AMB-21). Plasticizers that have shown promise include diethynyldiphenyl methane (DEDPM), phenylethynyldiphenyl methane (PEDPM), and mixtures thereof.

Resin	Weight Percent of AMB-21	Weight Percent of DEDPM	Weight Percent of PEDPM	Thermal History (Staging)	Viscosity @ 120 °C (cPs)	Solvent
1	50	50	-	Rotary Evaporation 100 °C, 30 min	300 to 1,000 (Scattered)	THF
2	60	40	-	*	~100	THF
3	70	30	-	*	~100	THF
4	80	20	-	*	>1,000	THF
5	70	30	-	Vacuum Evaporation 70 °C, 1 hr 90 °C, 1 hr	2,900	Acetone
6	70	15	15	*	2,100	Acetone
7	70	15	15	*	6,000	Toluene
8	70	15	15	Vacuum Evaporation 70 °C, 1 hr	15,000	Acetone
9	70	15	15	*	2,000	Toluene
10	100	-	-	Rotary Evaporation 70 °C, 1 hr	-	Acetone
11	70	30	-	*	2,400	Acetone
12	60	26.6	13.4	*	480	Acetone
13	60	31.6	8.4	*	480	Acetone
14	60	40	-	*	400	Acetone
15	60	35.8	4.2	*	550	Acetone
16	60	26.6	13.4	*	355	Acetone
17	60	26.6	13.4	Rotary Evaporation 70 °C, 1 hr 90 °C, 1 hr	355	Acetone
18	60	26.6	13.4	Rotary Evaporation 70 °C, 1 hr 90 °C, 1 hr 110 °C, 0.5 hr	-	Acetone
19	60	26.6	13.4	Rotary Evaporation 70 °C, 1 hr 90 °C, 1 hr 110 °C, 1 hr	384	Acetone
20	60	26.6	13.4	Rotary Evaporation 70 °C, 0.5 hr 110 °C, 1 hr	-	Acetone

These Formulations of AMB-21 with the plasticizers DEDPM and PEDPM include some that could be suitable for RTM and a few that are unsuitable for RTM because their viscosities are too high.

During RTM, the plasticizer molecules lower the viscosity of a resin. During the cure that follows RTM, when the plasticizing effect is no longer needed, the plasticizer molecules disappear via addition reactions, without evolution of volatiles. This is advantageous in that volatiles can give rise to undesired voids in the finished part. The cured resin has relatively high thermal stability. The glass-transition temperatures (T_gs) of polymerized matrix resins formulated and processed following this approach equal or exceed the T_g (≈300 °C) of AMB-21.

One potential drawback of this approach

is that the high degree of cross-linking in these resins can suppress ductility and induce a brittle failure under single-cycle or fatigue loading, or can cause microcracking during cure. Therefore, the development effort has included tradeoff studies to identify the formulations of RTM-processable resins with the best high-temperature stability and ductility. The table depicts some of the formulations investigated thus far. Composite specimens made from some of these resins have exhibited promising thermal and mechanical properties. These studies were continuing at the time of reporting the information for this article.

This work was done by Robert Kovar, Nelson Landrau, Margaret Roylance, and Thomas Tiano of Foster-Miller, Inc., for **Glenn Research Center**.

Inquiries concerning rights for the commercial use of this invention should be addressed to NASA Glenn Research Center, Commercial Technology Office, Attn: Steve Fedor, Mail Stop 4–8, 21000 Brookpark Road, Cleveland, Ohio 44135. Refer to LEW-16926.

Burn-Resistant, Strong Nickel Alloys

Precise control of alloy composition affords both burn resistance and strength.

Lyndon B. Johnson Space Center, Houston, Texas

Alloy	Alloying Element	Proportion of Alloying Element, Weight Percent	Pressure for Onset of Burning in Pure Oxygen	
			MPa	psia
Ni-Al	Al	1.0	>69	>10,000
		3.0	>69	>10,000
		5.1	>69	>10,000
		10.3	2.1	294
Ni-Fe	Fe	5.0	>69	>10,000
		10.0	>69	>10,000
		20.0	>69	>10,000
		30.0	>2.68	375
Ni-Cr	Cr	9.77	>69	>10,000
		19.9	>69	>10,000
		37.12	2.1	294
		50.1	3.4	476
Ni-Mn	Mn	1.98	>69	>10,000
		6.0	>69	>10,000
		9.9	>69	>10,000
		52.1	0.34	47.6
Ni-Si	Si	5.0	>69	>10,000
		10.7	>69	>10,000
Ni-Ti	Ti	1.04	>69	>10,000
		3.15	>69	>10,000
		5.01	>69	>10,000
		8.3	31	4,340
		25.9	0.14	19.6
		43.9	0.14	19.6

The Compositions of Nickel Alloys affect their ability to resist burning.

Investigators at the Johnson Space Center White Sands Test Facility (WSTF) have developed specifications of the amounts of alloying elements needed to increase the specific strengths of nickel alloys while consistently maintaining their burn resistance. The issue of burn resistance versus strength arises because pure nickel resists burning in pure oxygen at pressures up to >10^4 psia (>69 MPa), but does not have enough specific strength to satisfy the requirements for use in engineered structures.

The high burn resistances of nickel and of some nickel alloys make them attractive for some structural applications. These alloys can be used in such oxygen-enriched structures as hyperbaric chambers and spacecraft, where fires could have catastrophic results. Because the specific strength of pure nickel falls short of structural needs, elements with high specific strength and low burn resistance — such as aluminum and titanium — are alloyed with nickel. Unfortunately, prior to this investigation, large variations in burn resistance among batches of nominally identical commercial nickel alloys had been observed. For example, while one batch of a commercial nickel alloy was found to burn in pure oxygen at a pressure > 10^4 psia (>69 MPa), another batch was found to burn at a pressure <5 × 10^3 psia (<34 MPa). This inconsistency renders the use of commercial nickel alloys in oxygen-enriched structures problematic at best, disastrous at worst. The WSTF investigators sought to discover why this inconsistency occurs.

The investigators identified an inherent looseness in the composition ranges of commercially produced, high-temperature, high-strength nickel alloys, which makes the alloys more likely to burn in oxygen-rich atmospheres. Combustion occurs because the alloying elements that are not burn-resistant — aluminum, silicon, manganese, titanium, chromium, and iron — are used in varying quantities to form primary solid solutions with nickel. The investigators found that even small variations in alloying content can significantly affect burn resistance. For example, in preliminary tests on two batches of the nickel alloy Haynes 214, one batch burned at a pressure above >10^4 psia (>69 MPa) while the other batch burned at only 3 × 10^3 psia (≈21 MPa), yet both batches were within manufacturer's specifications. Further study led to the conclusion that the difference between the burn resistances of the two batches was attributable to looseness in the proportions of the alloying elements aluminum and chromium.

If the proportions of the alloying elements in nickel alloys were better regulated, the primary solid solution phases could retain both the burn resistance of pure nickel and the strength of the alloying elements. The investigators found that if elements are added in the quantities shown in the table, the specific strengths of nickel alloys can be increased without reducing resistance to burning. The findings of this investigation are expected to ensure that differences among the burn resistances of manufactured nickel alloys can be reduced, without adversely affecting the safety of individuals who live and work in oxygen-rich atmospheres.

This work was done by Joel M. Stoltzfus of White Sands Test Facility and Moti J. Tayal of Rockwell International for **Johnson Space Center**.

MSC-22698

Self-Temperature-Compensated Ceramic Strain Gauges

External temperature-compensation circuits are not needed.

John H. Glenn Research Center, Cleveland, Ohio

Ceramic static-strain gauges capable of generating mechanical-strain signals much larger than spurious thermal signals have been invented. These gauges are intended for use at temperatures from room temperature to 1,250 °C. Heretofore, external circuits have been used to provide temperature compensation for (that is, to correct for or suppress the spurious signals of) strain gauges. No such external temperature-compensation circuits are needed for temperature compensation of the present developmental strain gauges.

There are numerous potential uses for self-temperature-compensated strain gauges as the transducers of strain and pressure sensors in automotive and aerospace applications that involve temperatures >200 °C. At the present stage of development, it is not yet possible to construct a single gauge of this type that can operate over the entire temperature range from room temperature to 1,250 °C; instead, one can construct one gauge that functions from 100 to 800 °C and another gauge that functions from 900 to 1,250 °C. Development efforts continue and are expected to lead to publication in a journal.

This work was done by Otto J. Gregory of the University of Rhode Island for **Glenn Research Center**.

Inquiries concerning rights for the commercial use of this invention should be addressed to NASA Glenn Research Center, Commercial Technology Office, Attn: Steve Fedor, Mail Stop 4–8, 21000 Brookpark Road, Cleveland, Ohio 44135. Refer to LEW-16704.

Aerogels With Gradients of Density

Density gradients could be tailored to obtain desired properties.

NASA's Jet Propulsion Laboratory, Pasadena, California

Aerogels with gradients in density have been produced in experiments, as part of an effort to develop materials that will be used in outer space to capture particles traveling at high speeds for the STARDUST mission.

On Earth, aerogels with gradients of density could be used as lightweight materials with tailorable optical, acoustical, thermal, catalyst-support, or microelectronic-packaging properties. In addition to extremely low (and now optionally spatially varying) densities, aerogels have unique combinations of properties that make them economically competitive with other materials that would otherwise be used in the same applications.

One experimental aerogel exhibited a gradient of density from 5 to 50 mg/cm^3. Depending on the intended application, the gradient of density in an aerogel component could be tailored to obtain the desired corresponding gradient in the optical or acoustical index of refraction, optical or acoustical attenuation, permittivity, thermal conductivity, or other property or properties of interest.

This work was done by Steven Jones and Peter Tsou of Caltech for **NASA's Jet Propulsion Laboratory**. *Further information is contained in a TSP [see page 1].*
NPO-20485

Molded Plastic Simulated Landscapes

Simulated landscapes of Mars have been made of thermoplastic sheets molded to shapes derived from images of the Martian terrain. These simulated landscapes can be used to advantage in scientific experiments, simulations, educational displays, and other applications, in which unitary molded plastic sheets can be handled more easily and pose less risk of contamination than do simulated landscapes made of loose rocks.

Fabrication begins with the selection of terrestrial rocks with a distribution of sizes and textures representative of the terrain of interest. The rocks are arranged on the vacuum table of a thermoforming apparatus. A sheet of thermoplastic material (e.g., polycarbonate 1.58 mm thick) is heated to drive off moisture, then is heated further to its softening temperature. When at the softening temperature, the sheet is placed over the rocks, then vacuum is applied via the table to pull the sheet down over the rocks. Once thus formed to the shape of the rocks, the sheet is allowed to cool, then is taken off the table. Any rocks inadvertently captured in the molded sheet are removed.

This work was done by Joseph J. Kosmo of **Johnson Space Center**. *Further information is contained in a TSP [see page 1].*
MSC-22885

BLANK PAGE

Mechanics

Hardware, Techniques, and Processes

35 Surface Micromachined Silicon Carbide Accelerometers

Books and Reports

35 Update on Fuzzy-Logic-Enhanced Digital-PIV Software

BLANK PAGE

Surface Micromachined Silicon Carbide Accelerometers

These accelerometers could be valuable for diagnosis of engines.

John H. Glenn Research Center, Cleveland, Ohio

Surface micromachined silicon carbide accelerometers are undergoing development for eventual use in high-temperature environments like those inside turbines, internal-combustion engines, and other machines. These accelerometers would be used to measure vibrations indicative of deterioration of mechanical components; as such, they would be valuable diagnostic tools that could give advance warnings of failures or for the need to perform maintenance. They would even be small enough to fit into turbine blades.

Like similar accelerometers micromachined out of silicon, surface micromachined silicon carbide accelerometers are based on the concept of displacements of proof masses suspended on springs and they include electrodes for (1) capacitive sensing of displacements of proof masses and (2) electrostatic feedback for centering and for nulling displacements caused by relatively steady forces like those caused by gravitation and centripetal acceleration. The figure depicts an experimental surface micromachined silicon carbide accelerometer in which the proof mass (also called the "shuttle") is suspended at opposite ends by springs in the form of folded beams (pairs of beams joined at trusses). At each end, the outer two beams are attached to a substrate at four anchor locations.

The particular folded-beam structure offers low stiffness (and thus high sensitivity to acceleration) along both directions perpendicular to the nominal longitudinal axes of the beams and high stiffness (and thus low sensitivity to acceleration) parallel to the nominal longitudinal axes of the beams. If an accelerometer of this or a similar configuration were to be used to measure turbine-blade vibrations, then it would be mounted with the nominal longitudinal axis oriented in the radial direction to minimize the undesired response to centripetal acceleration. The folded-beam structure also helps to minimize the undesired differential thermal expansion between the substrate and the shuttle.

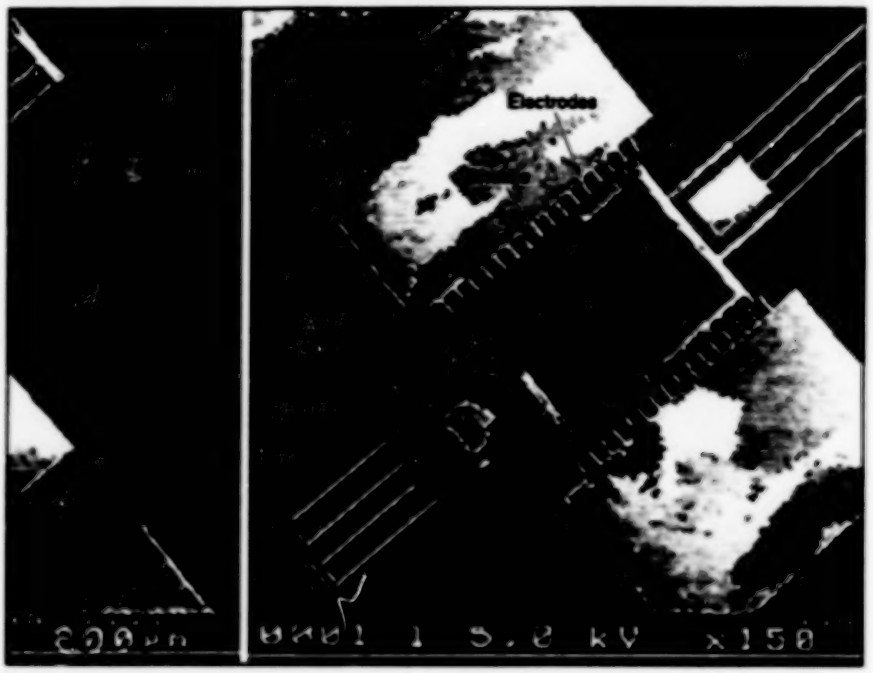

This Scanning Electron Micrograph shows the main stationary and moving components of an experimental surface micromachined silicon carbide accelerometer.

Electrodes for capacitive sensing of displacement and electrostatic actuation of the shuttle are located along the sides of the shuttle; two sets of these electrodes are on the shuttle and are interdigitated with adjacent sets of electrodes on the substrate. The gaps between the shuttle and the proximate substrate electrodes are typically 1 μm wide, and the electrode fingers are typically between 10 and 50 μm long. Inasmuch as capacitance between the substrate and shuttle is inversely proportional to the gap for small displacements, maximum sensitivity requires minimum gap. On the other hand, the gap must be made large enough to prevent touching of the substrate and shuttle electrodes at extreme excursions of the shuttle.

The main advantage of the silicon carbide accelerometers over silicon ones is the ability of any corresponding electronics (e.g., capacitance sensing circuits) to function at higher temperatures: Whereas silicon devices must generally be maintained at temperatures below 250 °C, silicon carbide devices can function at temperatures as high as 600 °C. Like silicon devices, silicon carbide devices can be fabricated inexpensively in batches with a high degree of repeatability.

This work was done by Russell G. DeAnna of the U. S. Army Research Laboratory for **Glenn Research Center**. *Further information is contained in a TSP [see page 1].*

Inquiries concerning rights for the commercial use of this invention should be addressed to NASA Glenn Research Center, Commercial Technology Office, Attn: Steve Fedor, Mail Stop 4–8, 21000 Brookpark Road, Cleveland, Ohio 44135. Refer to LEW-17002.

Books and Reports

Update on Fuzzy-Logic-Enhanced Digital-PIV Software

Two reports present additional information on the subject matter of "Software for Processing Data in Particle-Image Velocimetry" (LEW-16857) *NASA Tech Briefs*, Vol. 24, No. 1 (January 2000), page 26a. Like the cited prior article, both reports discuss the principles and the practical aspects of particle-image velocimetry (PIV), which is a method of determining a flow velocity field from images of small seed particles that are entrained in the flow and that are illuminated by laser pulses at known intervals of time. Also like the cited prior article, the reports describe PIVPROC — a user-friendly computer program that creates an interactive computing environment for displaying and processing PIV image

data and that employs fuzzy logic to maximize the amount and quality of velocity information extracted from the raw data. The cited prior article mentioned in passing that PIVPROC supports the combined use of cross-correlation and particle-tracking image-data-processing techniques to obtain high-quality velocity data over a wide range of particle-seeding densities; the two reports discuss this aspect of PIVPROC in more detail, with some emphasis on the fact that this combination of techniques yields velocities with the highest possible spatial resolution.

This work was done by Mark Wernet of **Glenn Research Center**. *To obtain copies of the reports, "Fuzzy Logic Enhanced Digital PIV Software" and "Particle Image Velocimetry Processing: PIVPROC," see TSP's [page 1].*

Inquiries concerning rights for the commercial use of this invention should be addressed to NASA Glenn Research Center, Commercial Technology Office, Attn: Steve Fedor, Mail Stop 4–8, 21000 Brookpark Road, Cleveland, Ohio 44135. Refer to LEW-17010.

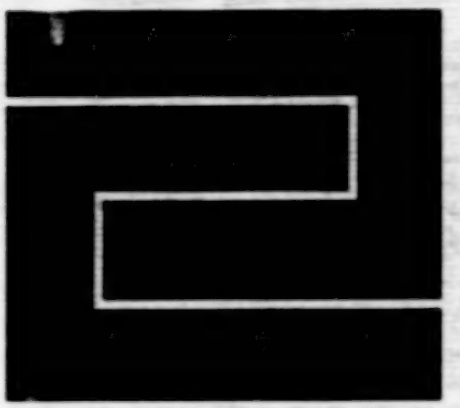

Fabrication Technology

Hardware, Techniques, and Processes

39 Bleaching by Laser for Marking Black Anodized Aluminum

BLANK PAGE

Bleaching by Laser for Marking Black Anodized Aluminum

Precise, intricate patterns can be formed at relatively low cost.

Lyndon B. Johnson Space Center, Houston, Texas

Irradiation by the beam from a CO_2 laser has been found to be an effective means of marking a black anodized aluminum surface. In general, this process works on any dark anodized surface. The beam is scanned over the surface to form a desired pattern. Depending on the circumstances, this technique could be an attractive alternative to painting, machine engraving, and etching; in particular, if there is a need to create a precise and/or intricate pattern, then this technique can satisfy that need in less time and at less cost while yielding better results. For this purpose, one uses a laser that is not powerful enough to cut the aluminum workpiece but is powerful enough to bleach the anodized surface to a nearly white appearance. The precise nature and degree of the bleaching depends on the specific aluminum-alloy/anodized-coating combination and on the parameters of the laser beam and scan. Tests at different laser power levels, scanning speeds, and numbers of pulses per unit length of scan must be performed on a sample of the particular anodized aluminum to find the combination of parameters that yields the best results.

The laser-scanning mechanism is driven by the output of a graphics program running under any Windows operating system. From the perspective of the program, the laser-scanning mechanism is merely a Windows printer. The pattern to be applied is drawn by use of the program, making allowances for the width of the laser beam (analogous to the diameter of a cutting or engraving tool). The drawing is then used to perform a test on a specimen of the anodized material to be marked. The resulting pattern is measured and any necessary corrections are made in the drawing data file. The revised drawing file is then tested as before, measured, and corrected as necessary. The cycle of test, measurement, and correction is repeated until the test and measurement indicate success.

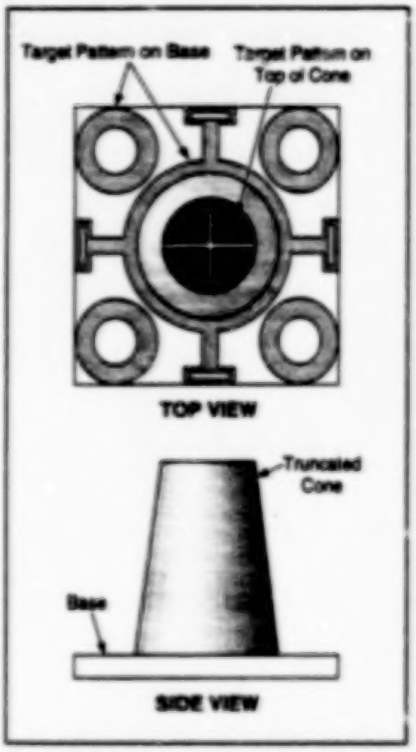

Target Patterns can be formed on the upper surface of the base and the top of the truncated cone by laser scanning.

The technique has been used to mark anodized aluminum docking targets shaped as truncated cones on square bases (see figure). In this application, there is a need for some additional process steps (beyond the basic steps described above). It is necessary to measure the anodized aluminum workpiece to determine the heights of the target pattern surfaces for proper adjustment of the laser. The corrected target-pattern drawing file generated as described above is used to generate three additional files: one for the perimeter of the base, one for the target pattern on the base, and one for the target pattern on top of the truncated cone. The base-perimeter file is used to laser cut a hole in a sheet of poly(methyl methacrylate) or other suitable material on the laser work table; this hole is used to position the workpiece. The other two files are used to control the laser of the base and top surfaces, respectively.

This work was done by Roger Megason, Herbert Mitchell, and Marvin Williams of **Johnson Space Center**. *Further information is contained in a TSP* *[see page 1].*

MSC-22848

BLANK PAGE

Mathematics and Information Sciences

Hardware, Techniques, and Processes

43 SIMON – School Internet Manager Over Networks

BLANK PAGE

SIMON – School Internet Manager Over Networks

This program is designed for managing access to the Internet for teachers and students.

Lyndon B. Johnson Space Center, Houston, Texas

School Internet Manager Over Networks (SIMON) is a software tool, exclusively for use on Macintosh computers, that is designed to provide access to, and management of, Internet information for teachers and students in kindergarten through twelfth grade. By eliminating the requirement for advanced system services typically provided by proxy servers (the computer tools of choice for access to the Internet), SIMON, which is available free on a NASA web site, has eliminated the related need for costly hardware servicing and system administration. Indeed, after installation, SIMON can maximize the overall utility of a user's local-area network (LAN), retrieve Internet information, and organize and present information to students. SIMON is not unique in the industry: several programs now commercially available perform a subset of functions that SIMON also performs. However, inasmuch as SIMON is uniquely tailored to the public-school milieu, it uses equipment commonly available to public schools, thereby reducing costs and serving as a more user-friendly product, relative to the other programs.

In these days of restricted funding, it is hardly surprising that public school systems are often short of money. Unfortunately, proxy servers, which are typically used as Internet-access tools, are available only on computers that are capable of hosting advanced system services (e.g., UNIX™ or Windows NT™). These systems are usually not financially viable for public school systems. Moreover, because proxy servers also demand a high degree of hardware support and system administration, the public school environment is not suited to these either.

SIMON overcomes these obstacles to access to the Internet. It does this by enabling the users for which it is uniquely tailored — public school systems — to use their own computers to retrieve Internet information, even when their computers are not directly connected to the Internet. More specifically, SIMON enables the users' system browsers to interact with mini-servers running on the users' own computers. Information requests are thus sent from a user's mini-server to the SIMON master server running on the computer connected to the Internet. By using the SIMON master server in this fashion, to funnel requests and distribute data across an LAN, teachers can control the content of the information and use stored library information to retrieve information even when the information is requested numerous times. Moreover SIMON is able to discriminate among users, recognizing two groups: teachers, who have special system privileges, and students. Teachers submit queries, which are answered with existing library documents and/or directly from Internet sources, and create the presentation documents, which are on file in the library. Students have access only to documents filed in the library. This arrangement enables teachers to manage materials used in the classroom and enables students to perform research and analyze information by use of Internet-based techniques.

As an Internet-access software tool, SIMON has few peers. Although it runs only on Macintosh computers, this one restriction is far outweighed by its benefits. SIMON features numerous search and retrieval functions (off-line searching, off-line browsing of search results, and downloading of web sites), lesson-building functions (off-line browsing of web sites, a lesson builder with web-page selector, and a lesson editor), and lesson-library-management functions (an off-line lesson library, automatic or manual lesson addition, and lesson-sharing utilities). By virtue of these advantages as well as ease of installation and use, SIMON will surely serve as a tool of the future — one that can satisfy a primary need in grades kindergarten through 12. Already used by the Department of Education, the user-friendly SIMON can be used in the development of curricula as well as to restrict access to the Internet.

This work was done by Robert O. Shelton of **Johnson Space Center**, *Stephanie Smith of Lincom Corp., and Dat Truong and Terry Hodgson of Space Applications International Corp. For further information, access* ***http://prime.jsc.nasa.gov***.

MSC-22898

END

06-26-00